universität wien

MASTERARBEIT | MASTER'S THESIS

Titel | Title

Cell division and storage compound synthesis: soil microbial community responses to drought and future climate scenarios

verfasst von | submitted by

Mona Lena Lauritz, B.Sc.

angestrebter akademischer Grad | in partial fulfilment of the requirements for the degree of

Master of Science (MSc)

Wien, 2024 | Vienna, 2024

Studienkennzahl lt. Studienblatt | degree programme code as it appears on the student record sheet:	A 066 833
Studienrichtung lt. Studienblatt | degree programme as it appears on the student record sheet:	Ecology and Ecosystems
Betreut von | Supervisor:	Univ.-Prof. Dr. Andreas Richter

Acknowledgements

First, I would like to thank my parents Andrea and Ralph, who made it possible for me to study and who have always supported me on my way and believed in me. I want to thank all my friends on the way, who had always an open ear for me. Thanks to Carla my bib-partner and Simon for his constant support in every aspect.

Special thanks to Andreas Richter, for giving me the opportunity to work on this project and supporting me with the writing. Thanks a lot, to Alberto Canarini, who did a great job by guiding me through all the lab procedures and helped me out with the statistical analyses.

Many thanks to all members of TER, the technicians for measuring my samples and the cleaning staff who always do a wonderful job!

Abstract

Microbial communities in soil play a crucial role in controlling biogeochemical processes. During their growth, microbes decompose organic matter and convert it into new biomass (new cells or storage products) which can either be stabilized within the soil or released back into the atmosphere as CO_2 through respiration. As climate change progresses, more frequent droughts, warming, and increased CO_2 concentrations will alter microbial living conditions, thereby affecting microbial growth and thus global carbon cycling. While most studies have focused on the individual effects of climate change factors on soil microbes, our understanding of the combined effects of cooccurring climate change factors remains limited. Furthermore, microbial growth is often measured as cell division, neglecting the fact that microorganisms can also allocate carbon to the intracellular synthesis of storage compounds, that can make up for a significant amount of cellular carbon. Here, we combine the analysis of cell division and storage compound synthesis and apply it in a multifactorial climate change experiment in a submontane grassland. We investigated the effects of a two-month summer drought (exclusion of rain) under ambient and future climate conditions (elevated temperatures of +3 $^{\circ}\mathrm{C}$ and elevated atmospheric CO_2 of +300 ppm above ambient). Growth rates and storage compounds synthesis were quantified by using ^{2}H-stable isotope probing. Specifically, we analysed the production rate of phospholipid fatty acid (PLFA) synthesis, together with the synthesis of bacterial polyhydroxybutyrate (PHB) and fungal and bacterial neutral lipid fatty acids (NLFAs, triglycerides). We demonstrate that drought strongly reduced bacterial growth, while fungal growth remained largely unaffected, except for arbuscular mycorrhizal fungi. Drought also strongly altered bacterial resource allocation, away from growth towards storage compound synthesis, except for

actinobacteria. Fungal growth, on the other hand, remained unaffected despite an increase in their storage compound synthesis, indicating a striking resistance of fungi to drought. Future climate conditions intensified drought impacts on bacterial growth but left fungal growth unchanged. Our findings highlight the importance of microbial storage compound synthesis and provide new insights into the physiological responses of soil microbes to a future, drier climate.

Zusammenfassung

Mikrobielle Gemeinschaften im Boden spielen eine wichtige Rolle bei der Steuerung biogeochemischer Prozesse. Während ihres Wachstums zersetzen sie organische Substanzen und wandeln diese in neue Biomasse um (neue Zellen oder Speicherprodukte), die anschließend im Boden stabilisiert oder während der Atmung als CO_2 in die Atmosphäre zurückgeführt werden kann. Mit dem Fortschreiten des Klimawandels führen häufigere Dürren, Erwärmung und erhöhte CO_2-Konzentrationen zu veränderten Lebensbedingungen für Mikroorganismen, was das mikrobielle Wachstum und damit den globalen Kohlenstoffkreislauf beeinflusst. Da die meisten Studien einzelne Effekte von Klimafaktoren auf Bodenmikroben berücksichtigen, bleibt das Wissen über die Folgen ungeklärt. Darüber hinaus wird mikrobielles Wachstum oft als Zellteilung verstanden, wobei übersehen wird, dass Mikroorganismen auch Kohlenstoff für die intrazelluläre Synthese von Speicherstoffen verwenden können, die einen erheblichen Anteil des Zellkohlenstoffs ausmachen können. In dieser Arbeit kombinieren wir die Analyse von Zellteilung und Speicherstoffsynthese und wenden diese in einem multifaktoriellen Klimawandel-Experiment in einem submontanen Grasland an. Wir untersuchten die Auswirkungen einer zweimonatigen Sommerdürre (Ausschluss von Regen) unter gegenwärtigen und zukünftigen Klimabedingungen (erhöhte Temperaturen von +3 $^{\circ}\mathrm{C}$ und erhöhte atmosphärische CO_2 Konzentrationen von +300 ppm). Wachstumsraten und Speicherstoffsynthese wurden durch ^{2}H-stabile Isotopenmarkierung quantifiziert. Insbesondere analysierten wir die Produktionsrate der Phospholipid-Fettsäuresynthese (PLFA) sowie die Synthese von bakteriellen Polyhydroxybutyraten (PHB) und neutralen Lipidfettsäuren (NLFA, Triglyceride) in Pilzen und Bakterien. Unsere Ergebnisse zeigen, dass Dürre das Wachstum von Bakterien stark reduzierte, während das Wachstum

von Pilzen weitgehend unbeeinflusst blieb, mit Ausnahme von arbuskulären Mykorrhizapilzen. Dürre veränderte auch stark die Ressourcenzuweisung bei Bakterien, weg vom Wachstum hin zur Synthese von Speicherstoffen, außer bei Actinobakterien. Das Wachstum der Pilze hingegen blieb unverändert, trotz einer Zunahme der Speicherstoffsynthese, was auf eine bemerkenswerte Resistenz der Pilze gegenüber Dürre hinweist. Zukünftige Klimabedingungen verstärkten die Dürreeffekte auf das Bakterienwachstum, ließen das Pilzwachstum jedoch unberührt. Unsere Erkenntnisse unterstreichen die Bedeutung der mikrobiellen Speicherstoffsynthese und liefern neue Einblicke in die physiologischen Reaktionen von Bodenmikroben auf ein zukünftig trockeneres Klima.

Table of Contents

1 Introduction

Atmospheric carbon dioxide (CO_2) concentrations have increased from approximately 278 parts per million (ppm) in 1750 during pre-industrial times [24] to 422 ppm in 2024 [76]. Human-induced deforestation and other land-use changes were main drivers of carbon release into the atmosphere, along with fossil fuel use for increasing energy consumption and lifestyle changes across regions [12]. All these carbon releases alter the natural carbon cycle, which circulates carbon between the atmosphere, the ocean, and the terrestrial biosphere [5] and between organic and inorganic carbon compounds. The projected increase in atmospheric CO_2 concentration is expected to cause the global average temperature to rise by 2 to 4 $^{\circ}\mathrm{C}$ by the end of this century [43]. This human made temperature rise increases the likelihood of extreme climatic events such as heat waves, heavy rainfall, droughts and tropical cyclones [12]. In Europe, climate scenarios predict a decrease in precipitation from May to October [18], which appears to intensify with global warming [66]. Considering the total amount of human CO_2 release since 1850, only 40 % has remained in the atmosphere, while the ocean and land acted as significant sinks, sequestering approximately 26 % and 32 %, respectively [22]. Also today, terrestrial ecosystems mitigate climate warming by absorbing carbon dioxide. However, their future sequestration potential under changing climate conditions is uncertain. Within terrestrial ecosystems, soils are the largest carbon (C) reservoir [37], storing nearly 3,000 Pg of C globally as soil organic carbon (SOC) [34]. Grasslands, which cover

almost 40 % of terrestrial biomes, significantly contribute to the global carbon pool, representing 25-34 % of the total carbon stock [83] [83].

The C input, cycling and loss in soils are determined by photosynthesis and respiration [71]. Plant biomass production is the primary source of SOC in soils, comprising the amount of carbon delivered through litterfall, root turnover, and root exudation [74]. The activity of soil microorganisms directly influences the SOC balance by decomposition and formation of soil organic matter [33, 80]. Soil microorganisms decompose soil organic matter by taking up organic matter and using it for their growth (i.e., secondary biomass production), maintenance and energy supply. Small oligomers and monomers of SOM are taken up directly while higher molecular weight compounds need to be depolymerised by extracellular enzymes [64]. Excess nutrients not required for microbial biomass production are mineralized, releasing nutrients for plant uptake [47]. The fraction of carbon used to build microbial biomass has the potential to enter a stable carbon pool as microbial necromass and contribute to the sequestration of SOC [38, 65]. Primary production is mostly nutrient-limited, while secondary production by heterotrophic microbial communities in soils are primarily limited by C and energy [71]. While plants can stimulate heterotrophic decomposition by providing energy-rich compounds, microbes set free excess nutrients for plant uptake. This relationship between plants and heterotrophs forms the basis for the functioning of ecosystems [71]. To determine the contribution of microbes to SOC formation it's important to distinguish between microbial catabolic and anabolic pathways [40]. To reflect soil carbon dynamics in a single metric, microbial carbon use efficiency (CUE) is calculated to elucidate the partitioning of assimilated carbon between microbial growth and respiration [74]. Efficient growth (high CUE) indicates a greater potential for soil organic C storage and thereby relatively low losses of soil organic C to the atmosphere through microbial respiration [40, 47], and vice versa. The link between SOC storage and CUE

is controversial, however. A high CUE might increase SOC storage due to an increase in microbial biomass [68], while other studies suggests that high CUE could stimulate SOC losses by increasing biomass and extracellular enzyme production, which enhances SOC decomposition [3]. Losses of SOC have the potential to accelerate global warming due to a positive climate feedback, while sequestration of CO_2 into soils as SOC may help to mitigate climate change [67]. The magnitude of CUE is closely related to the physiological conditions of microbes. Stressful conditions increase the demand for maintenance energy, thereby reducing growth and CUE [3]. Consequently, the stress tolerance and adaptive traits that microbes employ to cope with changing environment (life-history-strategy) can significantly influence the C turnover in soils and which part of the microbial community is active [64]. As climate change progresses, frequent droughts, warming, and increased CO_2 concentrations alter microbial living conditions. Elevated CO_2 levels are predicted to stimulate plant productivity and rhizosphere deposition, enhancing carbon allocation belowground [1]. This can have indirect effects on microorganisms, leading to increases in microbial biomass, respiration rates, microbial growth, and decomposition [1, 28]. Soil warming can directly stimulate or diminish microbial activity (depending on the starting temperature) and temperature-sensitive mediated processes, accelerating or decelerating organic carbon decomposition and microbial growth [3, 51, 79]. With elevated temperatures, evapotranspiration possibly increases thus reducing soil moisture. Conversely, elevated CO_2 level may increase soil moisture due to a reduction in stomatal conductivity resulting in lower evapotranspiration [1, 86]. Considering the combination of both, the increase in plant carbon inputs due to elevated CO_2 often dominate over temperature sensitivity of microbial activity [19, 20, 70]. As soils dry, pore water constituents become concentrated (dissolved nutrients, solutes, and toxicants) or may even precipitate, while the osmotic potential of the soil declines and the mobility of microbes diminishes [62, 63]. Additionally, drought directly affects plant litter composition as well

as the chemical composition of the microbial necromass, which are an important resource for microbes, as the plant and microbial communities change [7]. Consequently, as soil moisture decreases during drought, microbial access to resources diminishes, potentially slowing down microbial activity (i.e., respiration) [48], reducing microbial community growth, and increasing mortality [48, 62]. To cope with the temporal variability of environmental conditions, microbes can reduce their metabolic activity by entering a reversible state of dormancy [31]. This shift leads to changes in the active community composition, favouring more resilient microorganisms [63]. For instance, this adaptation may result in a higher fungi-to-bacteria ratio, as bacteria are more sensitive to drought than fungi. Additionally, there is often an increase in the abundance of gram-positive bacteria compared to gram-negative bacteria, owing to the former's thicker peptidoglycan cell wall, which offers greater protection [62]. However, transitioning into a dormant state increases energy and carbon requirements [55], causing microbes to reallocate resources away from cell division, resulting in lower growth rates.

The ability to synthesise products that affect ecosystem functioning are often overlooked when analysing microbial biomass growth. Many soil microorganisms can synthesize intracellular chemical compounds as intracellular chemical compounds in specific forms or compartments [49] to store energy, carbon or nutrients and helping them to avoid stress and mitigate unfavourable conditions. These storage compounds include nutrients like polyphosphate for phosphorus and energy [2] or cyanophycean for nitrogen [81]. Additionally, some compounds, such as triacylglycerides (TAG) and polyhydroxyalkanoates (PHA), store carbon exclusively. Both TAG and PHA are hydrophobic lipids stored as intracellular cytosolic lipid inclusions (lipid droplets) [49]. TAGs consist of three fatty acids esterified to glycerol stored are stored by bacteria and fungi, while PHAs are esterified polymers of 3-hydroxyfatty acids, and only found in bacteria [4, 42, 72]. Among PHAs, polyhydroxybutyrate (PHB) is a high-molecular-weight polyester

of ß-hydroxybutyrate [41]. Their degradation can drive ongoing metabolism, support maintenance at low growth rates, or facilitate the transition into or out of a physiological state like dormancy [42]. Furthermore, storage can reduce stochiometric imbalances between microbes and substrates by storing of a particular element, increasing their carbon use efficiency [39]. Thus, the ability of microbes to synthesize intracellular storage compounds has the potential to alter the composition of active community, creating shifts in the ecosystem-level C, energy, and nutrient flows [62]. The extend of intracellular storage compounds in soil may be driven by the soil fertility, as shown by a model in which the benefit and functional importance of nutrient and C storage increases with increasing C:nutrient ratio [42]. This indicates a strong link between element stoichiometry and storage. Nevertheless, storage could serve other roles beyond reserve C or nutrients, as they are accumulated during temporally variable stresses, e.g. cold-shock survival by protection from cellular oxidative stress [6], increased resistance during ethanol or heat stress [61] or osmotic stress response [46].

This shows that the benefits of storage are multifaceted and can enhance fitness in changing environments in various ways. Chapin III et al. (1990) defined a possible framework identifying two storage modes. One storage mode is surplus storage, based on the oversupply of abundant resources. This means that microbes store more C or nutrients than they require for growth and maintenance, and therefore have low opportunity costs. The second type is storage during limited resource availability, described as reserve storage, which occurs at the expense of other metabolic functions (occurring as fixed, taxon specific proportion of acquired C). While reserve storage is generally viewed as an investment for future reproduction [78], surplus storage is not limited to favourable conditions. It also includes storage during unfavourable times, such as when reproduction is constrained, or resource limitations occur despite the availability of another resource in excess [42]. In pure culture studies, both storage modes for PHA and

TAG were observed in microorganism under C-limiting and C-rich environmental conditions [35, 42]. A study of Mason-Jones et al. (2023) identified that, in soil microcosms, TAG storage followed the reserve mode, being independent of resource stoichiometry, while PHB storage responded dynamically to shifts in resource stoichiometry, indicating a surplus strategy. Since both compounds can provide C storage and mobilization, compound specific storage strategies are not necessarily expected. However, this study showed that storage can make up a significant pool of the microbial biomass not only under C-replete conditions, but also when C availability is limited. As storage compounds in microbes are dynamic and do not always reflect immediate environmental conditions but rather long-term storage in individual microorganisms [42], therefore its essential to consider the time scale of storage synthesis, remobilisation and microbial growth in relation to resource fluctuations [40].

The partitioning of carbon that microbes assimilate between cell division and the synthesis of storage compounds is a vital physiological process, playing a crucial role in microbial resistance strategies, particularly for survival and recovery under adverse conditions. However, little is known about how microbial growth and storage compound synthesis might change under future climatic conditions. Given that elevated CO_2, elevated temperatures, and climatic extremes, such as drought, usually co-occur [43], and considering the rarity of field experiments that address all these factors concomitantly [60], the objective of this research was to simultaneously quantify microbial growth rates (cell division) and storage compound synthesis (neutral lipid fatty acids, polyhydroxybutyrate) during a simulated summer drought in a managed grassland, both under current and future climate conditions (i.e., +3 $^{\circ}\mathrm{C}$ warming and +300 ppm CO_2).

We addressed the following research questions:

1. How does drought affect the microbial carbon allocation to cell division and storage compound synthesis?

2. Do microbial growth and storage product synthesis respond differently to drought under future climate conditions (+3 $^{\circ}C$ warming and +300 ppm CO_2) than under ambient conditions?

To our knowledge, this study is the first to quantify the combined effects of future climate conditions and drought on microbial growth and the synthesis of intracellular storage compounds. In a multifactorial field experiment ("ClimGrass") we analysed the effect of a two-month summer drought under ambient and future climate conditions (i.e., elevated temperatures of + 3 $^{\circ}C$ above ambient, and elevated atmospheric CO_2 of + 300 ppm above ambient) and compared them with the reference conditions. We approached growth (cell division) via PLFA stable isotope probing with Deuterium-enriched water (^{2}H-PLFA-SIP) based on the water vapour equilibration technique [15]. We assessed microbial storage product synthesis in the same labelling experiment by analysing by the incorporation of ^{2}H into neutral lipid fatty acids (NLFA) for fungi and bacteria, and polyhydroxybutyrate (PHB) for bacteria.

2 Methods

2.1 Study area

The study is part of ClimGrass, a multifactorial climate change experiment, managed by the Agricultural Research and Education Centre (AREC) Raumberg-Gumpenstein. The soil samples were collected on sub-montane grassland site classified by a Cambisol with a loamy sand texture (pH: $\sim$ 5.5) and located in the middle of Austria, in the Styrian Enns Valley ($47°29'38''$N, $14°6'3''$E, 710 m a.s.l.). The prevailing climatic conditions are characterized by an average annual temperature of 8.5 $°C$ and average annual precipitation of 1077 mm. On 54 test plots with a size of 16 m² each, the effects of future climate conditions on grassland soils have been continuously investigated since 2014.

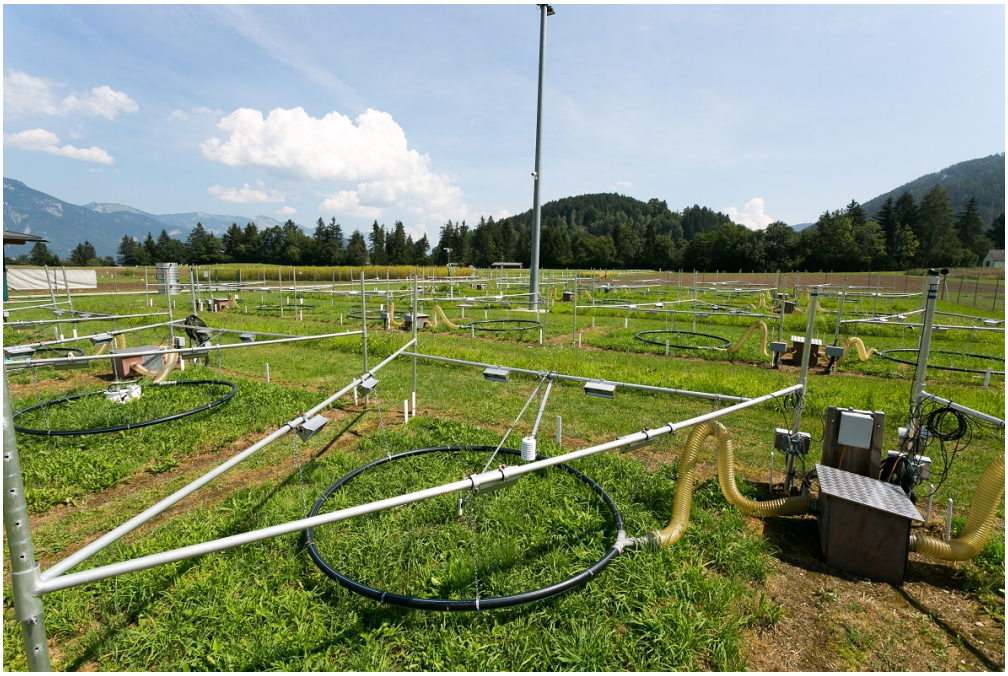

Figure 1: Experimental setup: miniFACE ring is used for CO_2 fumigation (+300 ppm) and to manipulate air temperature (+ 3°C) infrared heaters fixed on a triangular frame. Figure from [58] © HBLFA Raumberg-Gumpenstein.

Six treatments were established through the combined effect of warming and carbon dioxide enrichment including three different temperature (ambient, +1.5 $^{\circ}$C and +3°C) and CO_2 levels (ambient, + 150ppm and +300ppm). Manipulations of atmospheric CO_2 concentrations were done through a miniFACE free air CO_2 enrichment system, whereas atmospheric temperature was manipulated using infrared heaters (Figure 1). In addition, automatic adjustable rainout shelters were used to simulate summer drought events by temporarily withholding precipitation. Site management includes mowing three times a year and mineral fertilization (90kg N ha^{-1} a^{-1} as NH_4NO_3, 65 kg P ha^{-1} a^{-1} as $Ca(H_2PO_4)^2$ and 170 kg K ha^{-1} a^{-1} as K_2O), which corresponds approximately to the amount of NPK removed by biomass harvest, in order to replicate local farming practices.

2.2 Study design and soil sampling

Within this experiment, 16 plots of the ClimGrass site were examined to study the potential effects of climate change and drought. This includes four different treatments: (1) ambient climate conditions, (2) ambient climate conditions in combination with drought, (3) future climate conditions, and (4) future climate conditions in combination with drought. The future climate conditions in the experiment are simulated by a concomitant increase of temperature by 3°C and elevated atmospheric CO_2 level of +300 ppm above ambient. In addition, summer drought was experimentally induced for two months, starting on 25th of May 2023 and ended with a rewetting on 26th July 2023. Soil samples were harvested four times during this study period. The initial harvest on 24th of May 2023 (May) started after the first mowing and before start of drought. After one month of drought the second harvest took place on the 27th of June 2023 (June). For the third harvest, samples were collected on the 26th of July 2023 (July) after the second mowing. The last harvest was conducted on the 1st of August 2023 (Aug), after one week of rewetting. At each time point, 2 soil cores (2 cm diameter) from the top 10 cm of each treatment were collected and mixed to reduce plot-level heterogeneity. Soil was sieved through a 2 mm sieve and rocks, roots and plant leaves were removed.

2.3 Lab work

In this study, we measured the following variables:

- Phospholipid fatty acids (PLFA) were analysed as a proxy for the biomass of different microbial groups
- Neutral lipid fatty acids (NLFA) and polyhydroxybutyrate (PHB) as microbial

storage and bacterial storage compounds, respectively.

In addition total microbial biomass was estimated by the chloroform fumigation extraction method. Soil water content was measured on 5 g fresh soil dried overnight (12h) at 105 °C. In order to measure production rates of PLFA, NLFA and PHB we used the ^{2}H-vapor-SIP method [13], and followed the incorporation of ^{2}H into this compound classes. I discuss each analysis in detail below.

2.3.1 Chloroform fumigation extraction

To determine total microbial biomass C and N, chloroform fumigation extraction was conducted [77]. This was done by preparing two aliquot of 2 g of fresh weight per sample. One of the two aliquots of each sample received 15 ml of 1 M potassium sulphate (KCl) and was shaken for 30 minutes. Afterwards the extracts were filtered through glass wool filters (carbon and nitrogen free) and were frozen at -20°C until further analyses. The other aliquots were fumigated by placing an open glass vial containing 1 ml chloroform into a scintillation glass vial containing 2 g of the soil aliquot. With this approach we avoid direct contact between the chloroform in the liquid phase and the soil sample. The scintillation vial was sealed airtight, and the samples were fumigated for 48 h. The second fumigated aliquot was then extracted in the same way as the non-fumigated aliquot. To analyse the C and N content of the produced extracts, the samples were analysed via a TOC/TN analyser (TOCVCPH E200V/TNM-122V; Shimadzu, Vienna, Austria). Microbial biomass carbon (MBC) was calculated as the difference in TOC concentrations between chloroform fumigated and non-fumigated extracts and corrected using a factor of 0.45 [30]. Microbial biomass N (MBN) was calculated as the difference in TON concentrations between chloroform fumigated and non-fumigated extracts and corrected using a factor of 0.54 [10].

2.3.2 Soil ^{2}H-vapor-equilibration to estimate the production rate of PLFAs, NLFas, and PHB

The incubation started $\sim$ 24 h after sampling. Samples were incubated according to the ^{2}H vapor equilibration method as described in Canarini et al. (2020) for ^{18}O water. In this method, soil samples are weighed into a vial and labelled water (referred to as "source water) is added without direct contact with the soil. The vial is sealed allowing the source water and the soil water to equilibrate its isotopic composition via equilibration of the water. Two set of samples were prepared, either subjected to source water containing ^{2}H (deuterium) labelled water or water at natural abundance isotope concentrations.

For this, 4 g of soil samples were weighed into 50 ml head space vials. The source water was placed on the soil sample by using an additional smaller vial without direct contact with the soil.

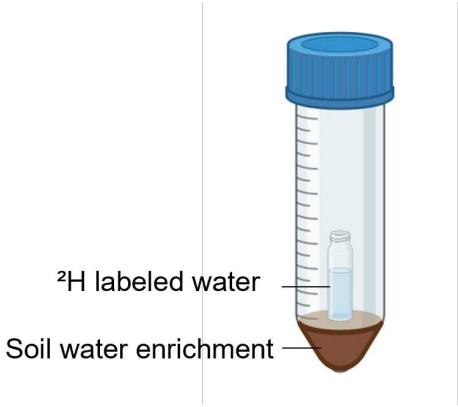

Figure 2: Setup of deuterium vapor equilibration incubation. Source water placed on top of soil without direct contact within an airtight tube. By source water evaporation, the soil water to equilibrate its isotopic composition**.**

We calculated the amount of ^{2}H into the source water to reach a final soil water enrichment of about 4 at%, which would expose soil microbes to an average soil water enrichment of around 2at% during the 48hours of the incubation. After

placing the water source in the vial, the head space vials were sealed with airtight rubber septa and incubated at field temperatures for 48 hours (May: ambient (+ drought) = 17°C, future climate (+ drought) = 20°C; June, July, Aug: ambient (+ drought) = 20°C, future climate (+ drought) = 23°C). To monitor the ^{2}H enrichment of the soil water over time, we randomly selected several samples (two for each treatment) and prepare them as described above. From this we collected aliquots of the remaining isotopically labelled water after 4, 8 and 24 h of incubation. In addition, we collected the water at the end of the 48 h incubation for all the samples, to calculate the incorporation of ^{2}H into soil water as described in Canarini et al. (2020). The ^{2}H enrichment of the soil water is used to calculate PLFA/NLFA and PHB production and ultimately microbial growth, and the average ^{2}H enrichment of soil water needs to be calculated across the incubation time (48 h) to account for the temporal dynamics of isotope equilibration of soil water. The collected water samples were analysed for ^{2}H enrichment using platinum catalysed equilibration of ^{2}H in H_2O with H_2 gas by a Gasbench II headspace sampler connected to a Delta V Advantage isotope ratio mass spectrometer (Thermo Fisher, Bremen, Germany). The resulting curves represent the equilibration of the ^{2}H labelled external water via the vapor phase with soil water, and were fitted with a negative exponential function (eq. 1) as described in Ingraham, and Criss:

$$^{2}\mathrm{H}_{soilwater,at\%} = {}^{2}\mathrm{H}_{48h,at\%} + ({}^{2}\mathrm{H}_{initial,at\%} - {}^{2}\mathrm{H}_{48h,at\%})(e^{-bt}) \tag{2.1}$$

where $^{2}\mathrm{H}_{48h,at\%}$ and $^{2}\mathrm{H}_{inital,at\%}$ represent the ^{2}H at% of the water after 48 h incubation and at time point 0, and *b* represents a soil specific coefficient that was generated by fitting the *nls()* function in R. We used the values (and *b*) to generate a prediction of the soil water isotopic enrichment as was described for ^{18}O demonstrated in Canarini et al. Finally we calculated the integral of this function by using the function *integrate()* of the R package “pracma” [9] between

time 0 and 48 hours. This integral was divided by 48 hours to generate an average isotopic enrichment of soil water for each treatment.

Soil samples subjected to 48hours incubations were transferred to a new vial and immediately frozen in dry ice before being stored at -20°C for further analysis. Microbial respiration was determined by measuring the CO_2 concentration in the headspace vial right after the application of ^2H enriched water and 48 h after the incubation using an infrared gas analyser (EGM4, PP systems).

2.3.3 Extraction of Phospho - and Neutral Lipid Fatty Acids

To determine microbial growth and active community composition PLFA were extracted from incubated soil (deuterium labelled and natural abundance controls). Incorporation into NLFAs was used to quantify the investment in intracellular lipid storage. Lipid extraction was based on a modified version of a high throughout method as described in [23]. For this, 2 g of freeze-dried soil samples were used to perform a two-phase extraction [8]. First, total lipids are obtained by applying a monophasic mixture of citrate buffer: methanol: chloroform (1:2:0.8). Then the total lipids were fractionated by solid phase extraction, whereby the samples are applied to a silica column (Phenomenex, Strata SI-1 Silica, 55 µm, 70 A). To collect different lipid fraction, solutions with a different polarity are sequentially added and collected in different vials. The NLFA fraction is eluted with chloroform containing 2% of ethanol. PLFA are collected with a chloroform: methanol: water mixture (5:5:1), after silica columns are washed with acetone to exclude glycolipids. The collected lipid fractions are derivatised via alkaline methanolysis to produce fatty acid methyl esters (FAME). For quantification, an internal standard fatty acid methyl ester 19:0 (nonadecanoic acid) is added before derivatization and samples are stored at -20°C until measurement.

2.3.4 Extraction of Polyhydroxybutyrate (PHB)

The synthesis of PHB as another intracellular microbial storage compound was quantified by measuring the incorporation of deuterium into PHB. Here, 2 g of freeze-dried soil was used and extracted via an accelerated solvent extractor (Thermo Scientific Dionex ASE 350 Accelerated Solvent Extractor). A mix of dichloromethane: methanol (5:2) was used as solvent. The recovery efficiency of this method was validated adding pure PHB to soil samples from the same site; the recovery rates determined in this way were 94%. After extraction samples were dried under a constant stream of N_2 at 45°C. Based on a modified version of [82], samples were derivatised via acidic alcoholysis producing butyl esters. Along samples, an external standard dilution series was added using a purchased PHB standard (2 mg ml^{-1}) to quantify PHB within samples. Dried samples were rewetted by adding butanol and HCl (32 %) and left in a dry bath at 100°C for at least 6 h. During the incubation, samples were shaken every hour. After 6 hours samples were removed and after cooling down were washed twice with water. To ensure accuracy during measurement, undecane diluted in hexane (1:10) was added as internal standard for quantification.

2.3.5 PLFA, NLFA and PHB measurement

PLFA, NLFA and PHB samples were quantitatively analysed to determine incorporation. This was done by using a Trace GC Ultra connected by a GC-IsoLink to a Delta V Advantage Mass Spectrometer (all Thermo Fisher Scientific). The identification of fatty acids and PHB, was achieved on a GC (7890 B Agilent Technologies, USA) connected to a time of flight (TOF) MS (Pegasus BT, LECO, USA) with the same program as described below. Fatty acids were identified using mixtures of bacterial and fungal FAMEs (Bacterial Acid Methyl Ester CP Mixture (Matreya LLC, State College, PA, USA) and 37 Comp. FAME Mix (Su-

pelco, Bellefonte, PA, USA)), and quantified against the internal standard (19:0). For PHB, the derivatized external standard (corrected by the internal standard) was used to quantify the PHB of each sample.

Samples were injected in splitless mode (injector temperature 300 ℃) and separated on a DB5 column (60 m × 0.25 mm × 0.25 µm; Agilent, Vienna, Austria) with 1.2 ml He min-1 as the carrier gas (GC program: 1 min at 80 ℃, 30 ℃ min-1 to 150 ℃, 1 min at 150 ℃, 4 ℃ min-1 to 230 ℃, 30 min at 230℃, 30 ℃ min-1 to 280 ℃ and 19 min at 280 ℃). The H3 factor (correction for abundance of the trihydrogen ion H3+) was defined based on multiple injections of reference hydrogen gas before each sequence and was very stable over time (3.64 ± 0.05 ppm/nA). Sample δ2H values were normalized to the VSMOW scale using the slope and intercept of measured and known values of isotopic standards. These were individual and fatty acid mixes of USGS70 and USGS72 (Arndt Schimmelmann, Indiana University) measured before and after each measurement run, as described above, and ranging from δ2H -183 ‰ to 384 ‰. Offsets between measured and known values for these standards were used to correct for any drift over the course of the sequence or any isotope effects associated with peak area or retention time. The standard deviation for these standards averaged 4‰ and the average offset from their known values was 27 ‰.

We used the markers 18:1ω9cis, 18:2ω6,9 and 18:3ω6,9,12 to estimate fungal biomass [23]. For gram-positive bacteria we used the sum of a15:0, a17:0, i15:0, i16:0, i17:0 markers and for the actinobacteria the markers 10Me17:0 and 10Me18:0. For gram-negative bacteria we used the markers 16:1ω7, 18:1ω5, 19:1ω9 and cy17:0. Fungi to bacteria ratio was calculated as the ratio between the fungal biomass and the sum of gram positive (including actinobacteria) and gram negative. We used the markers 16:1ω5 as indicative of arbuscular mycorrhizae fungi but kept separated from the other fungal biomarkers. The

remaining markers including 17:0Me, 18:1ω9trans, 16:0, 17:0, 18:0, 20:0 cannot be exclusively assigned to bacterial or fungi and markers with double bond position which could not be chromatographically resolved (16:1ωX, 17:0Me, 17:1ωX, 19:1ωX), were assigned to the general PLFA marker group.

2.3.6 Calculations

The following calculations for biomass specific PLFA, NLFA and PHB production are based on [13]. The amount of freshly C produced during the incubation period in each fatty acid ($C_{FA,produced}$, ng C per g soil dry mass) or PHB ($C_{PHB,produced}$, ng C per g soil dry mass) was calculated by using

$$C_{FA,produced} = \frac{\Delta\ ^2\mathrm{H}}{^2\mathrm{H}_{soilwater}\ aw} C_{FA} \tag{2.2}$$

$$C_{PHB,produced} = \frac{\Delta\ ^2\mathrm{H}}{^2\mathrm{H}_{soilwater}} C_{PHB} \tag{2.3}$$

For this, the difference between natural occurring amount of deuterium and the measured amount of deuterium after the incubation ($\Delta\ ^2\mathrm{H}$, at %) was divided by the amount of deuterium labelled in soil water ($^2\mathrm{H}_{soilwater}$, at %) estimated by the equilibrium curve. To account for the uncertainties in the growth rates due to the microbial assimilation efficiency of deuterium in fatty acids, aw = 0. 71 [16], was added. The specific internal standard (FA: 19:0, PHB: undecane) was used to calculate the C concentration of each fatty acid or PHB (C_{FA}, C_{PHB}, ng C per g soil dry mass). With this, microbial biomass production rates of PLFA's , NLFA's and PHB's of each sample were determined. Here as an example for PLFA

$$G_{PLFA} = \left(\frac{C_{PLFA,produced}}{C_{PLFA}} MBC \right) / t \tag{2.4}$$

According to the equation, the relative amount of freshly produced C of PLFAs ($C_{PLFA,produced}$, ng C per g soil dry mass) per total C of PLFAs (C_{PLFA}, ng C per g soil dry mass) was multiplied by the total microbial biomass C (MBC) to calculate the biomass production within the incubation time. The production rate (G_{PLFA}, ng C per g soil dry mass per hour) was calculated by dividing the production by the incubation time. Finally, mass specific production ($G_{PLFA,MS}$, mg C per g C per hour) was calculated relative to the total microbial biomass C (MBC) by using

$$G_{(PLFA,MS)} = \frac{G_{PLFA}}{MBC} \tag{2.5}$$

Moreover, the mass specific production rates of PLFA and NLFA were calculated separately for specific microbial groups. For this, the production rate of a specific microbial group were summarized $C_{FA,produced}$ relative to C_{FA} of a specific microbial group and divided by the incubation time. The group specific production of PHB or NLFA in relation to their mass specific growth rate was calculated by dividing the production rate of storage compound (PHB or NLFA) by the mass specific PLFA production rate of bacterial or fungal marker, respectively. Here is an example for gram negative NLFA production ($G_{rel\ NLFA,gram-}$)

$$G_{(rel\ NLFA,gram-)} = \frac{G_{NLFA,gram-}}{G_{PLFA,gram-}} \tag{2.6}$$

The microbial respiration rate ($C_{Respiration}$, ng C per g soil dry mass and per hour) was quantified by the amount of produced CO_2 during the 48-hour-lasting incubation. With this, the C allocated to microbial biomass production (G_{PLFA}, ng C per g soil dry mass per hour) and respired C is described as the total C

uptake (C_{Uptake}, ng C per g soil dry mass per hour).

$$C_{Uptake} = G_{PLFA} + C_{Respiration} \tag{2.7}$$

To gain insight into the efficiency of the microbial community in utilizing the uptaken carbon, the microbial carbon use efficiency (CUE) was calculated as the relative partitioning of microbial growth (G_{PLFA}, ng C per g soil dry mass per hour) and carbon uptake (C_{Uptake}, ng C per g soil dry mass per hour):

$$CUE = \frac{G_{PLFA}}{C_{Uptake}} \tag{2.8}$$

2.3.7 Statistical analysis

All statistical analyses were executed in R studio software version 4.3.2 [75]. Results with a p-value $\leq$ 0.05 were considered as significant. The corresponding graphs were plotted using R package “ggplot2” [84]. Three data points (sample ID: AD4, F1 and F2) were identified as outlier by using cook’s test and were removed from the dataset in August.

To obtain a general overview of the total C allocation in our data, the total amounts and relative C allocation were plotted. The R packaged “nlme” [56] were used to assess linear mixed effect models to test treatment specific differences per month. All models were tested for the effects of climate (ambient and future climate) and drought (drought and no drought) as well their interaction. To account for variations between the 16 investigated plots, the plot variability was added as random factor. Thereby, mass specific respiration, CUE and PHB production were compared on a community-specific level, while mass-specific microbial growth, synthesis of NLFA and microbial abundance were additionally

analysed on a group-specific level. The model assumptions (normal distribution and heteroscedasticity) were tested and checked visually and if necessary, the dependent variable was logarithmically or quadratically transformed. To test for the main effects, the models were tested by using a two-way ANOVA. In order to correct for the false discovery rate (FDR) due to the high number of tests, we adjusted the p-values by using the Benjamini-Hochberg ("BH") with the R function *p.adjust()*. Principal component analyses of relative PLFA abundances and growth rates were assessed via the function 'PCA' of the package 'FactoMineR' [36] and scores were normalized by setting scale = TRUE. Statistical significance of relative PLFA abundances and growth rates between treatments was assessed via PERMANOVA with the function 'adonis' of the 'vegan' package [52] using Euclidean distances. For both PCA and PERMANOVA data was split by time.

3 Results

3.1 Microbial carbon pools

The total soil microbial biomass carbon (MBC) in all plots (including ambient-, future climate- and drought treatments) quantified via the chloroform fumigation extraction method, was on average 489 μg C g^{-1} DW, with MBC being lowest in July (438 μg C g^{-1} DW) and highest in August (543 μg C g^{-1} DW) (Figure 3).

The absolute quantities of PLFAs remained constant (25-27 μg C g^{-1} DW) over the months, while the storage compounds varied. On average NLFA quantities ranged from 57 μg C g^{-1} DW in May and August to 78 μg C g^{-1} DW in June and July. The absolute PHB quantities were lowest in May and June with 7 μg C g^{-1} DW and increased in August to 14 μg C g DW^{-1}. On average representing 21% of the of total microbial biomass C, including 5.4% PLFA and 15.6% of storage compounds.

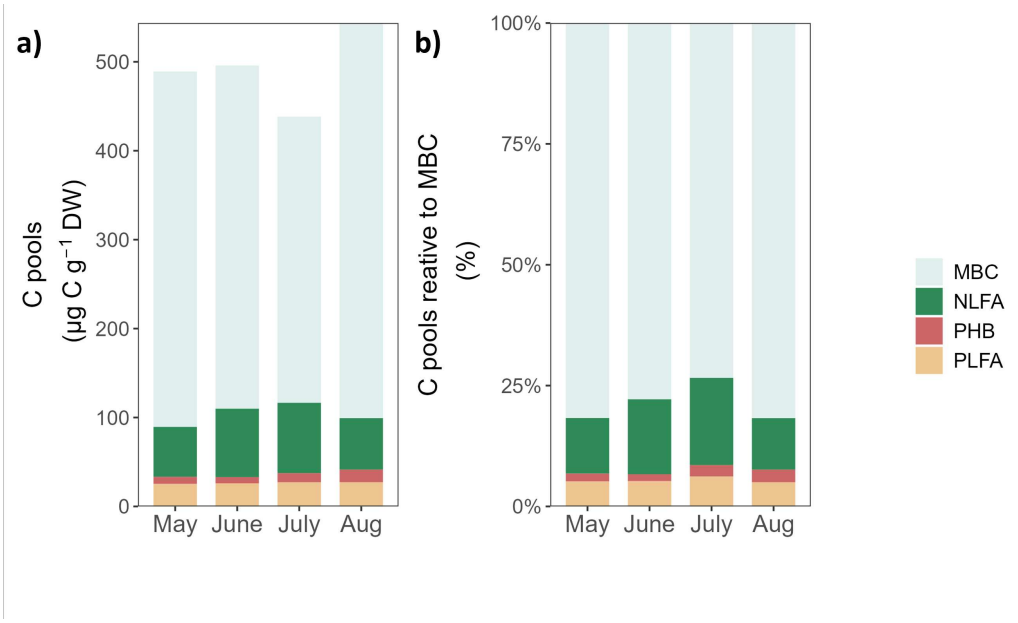

Figure 3: Microbial carbon pools within the total microbial carbon (MBC). Here we represent a) the total quantities (μg C g^{-1} DW) and b) the relative proportion (%) of PLFA, NLFA and PHB within the MBC. The colours indicate the compounds, and the height of each segment represents its contribution to the total MBC. The MBC was corrected for incomplete extraction by using a factor of 0.45.

When analysing the temporal dynamics of absolute quantities (μg C g^{-1} DW) during drought and future climate, PLFAs and PHB remained not significantly different in both scenarios (Figure 4 b d, Table 1). Although MBC was unaffected by drought, NLFAs were significantly reduced after drought in August when the soil was rewet (Figure 4 c). Under future climate conditions, NLFAs only increased in May, before these years summer drought. MBC showed no initial effect under future climate conditions but increased after the drought (August) when the soil was rewet (Figure 4 a).

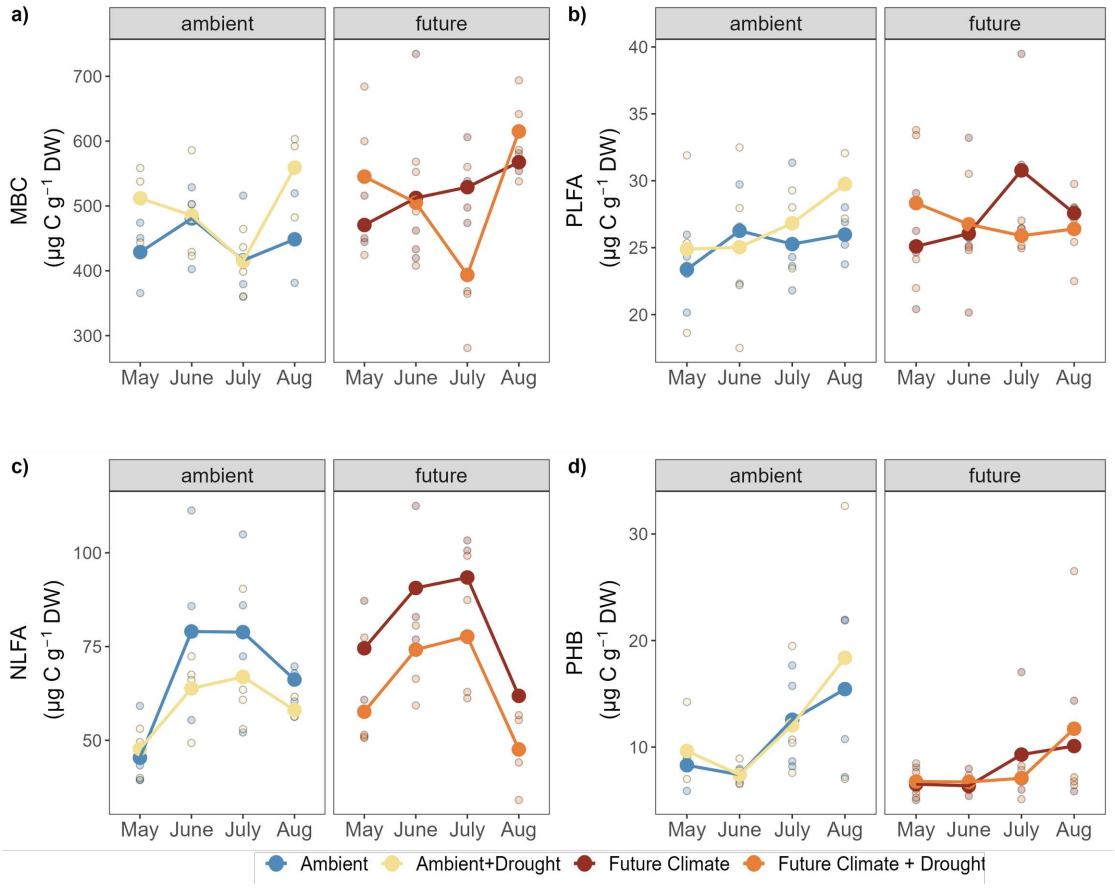

Figure 4: Total amounts of MBC, PLFAs, NLFAs and PHB. Quantities were measured at 4 time points (May [25.05.]: initial conditions; June [26.06.]: beginning of drought period; July [27.07.]: peak drought; August [01.08.]: rewetting) under 'ambient' and 'future' climate (eT and eCO2) conditions. Each line plot is coloured after the specific treatment, representing the mean at each time point.

Table 1: Effect of future climate (C), drought (D) and their interaction (I) on absolute quantities (μg C g^{-1} DW) of microbial biomass carbon (MBC), PLFAs, NLFAs and PHB. The p-values were derived from linear mixed effect models for each time point (May [25.05.]: initial conditions; June [26.06.]: beginning of drought period; July [27.07.]: peak drought; August [01.08.]: rewetting). The p-values were adjusted (Adj. p) using "Benjamin-Hochberg" method. Significant p-values (<0.05) are represented in bold. See full report in Table 8.

		May	June	July	August
MBC	*C*	0.4135	0.9767	0.2621	**0.0261**
	D	0.0867	0.9767	0.1469	0.0524
	I	0.7382	0.9767	0.1469	0.3862
PLFA	*C*	0.4386	0.9099	0.3673	0.5688
	D	0.4386	0.9099	0.4233	0.3698
	I	0.7184	0.9099	0.2668	0.2214
NLFA	*C*	**0.0045**	0.2973	0.2372	**0.0286**
	D	0.1761	0.1772	0.2372	**0.0286**
	I	0.1077	0.9429	0.8325	0.4489
PHB	*C*	0.0869	0.1482	0.1035	0.6640
	D	0.6055	0.6914	0.7031	0.9064
	I	0.6055	0.6914	0.7031	0.9091

3.2 Mass-specific microbial growth, respiration, and carbon use efficiency

We analysed mass specific growth, mass specific respiration rates (mg C g $^{-1}$ microbial C h^{-1}) and calculated Carbon Use Efficiency (CUE) of the microbial community. The impact of drought (during June and July) significantly reduced all physiological parameters of the microbial community (Figure 5, Table 2). In July, drought reduced mass-specific respiration by 53% and 60% under ambient and future climate conditions, respectively (Figure 5 a). The effect of drought on

overall mass-specific growth was larger with reductions of 67% and 80% under ambient and future climate conditions, respectively (Figure 5 b), leading to a decline in CUE by 22% under ambient and by 36% under future climate (Figure 5 c). With rewetting in August, all physiological parameters recovered to the level observed in control conditions. Future climate had no significant effects on microbial physiology compared to ambient conditions during drought, however future climate conditions increased on average biomass-specific respiration by 24% and biomass-specific growth by 41% before this year's summer drought (May) (Figure 5 a b).

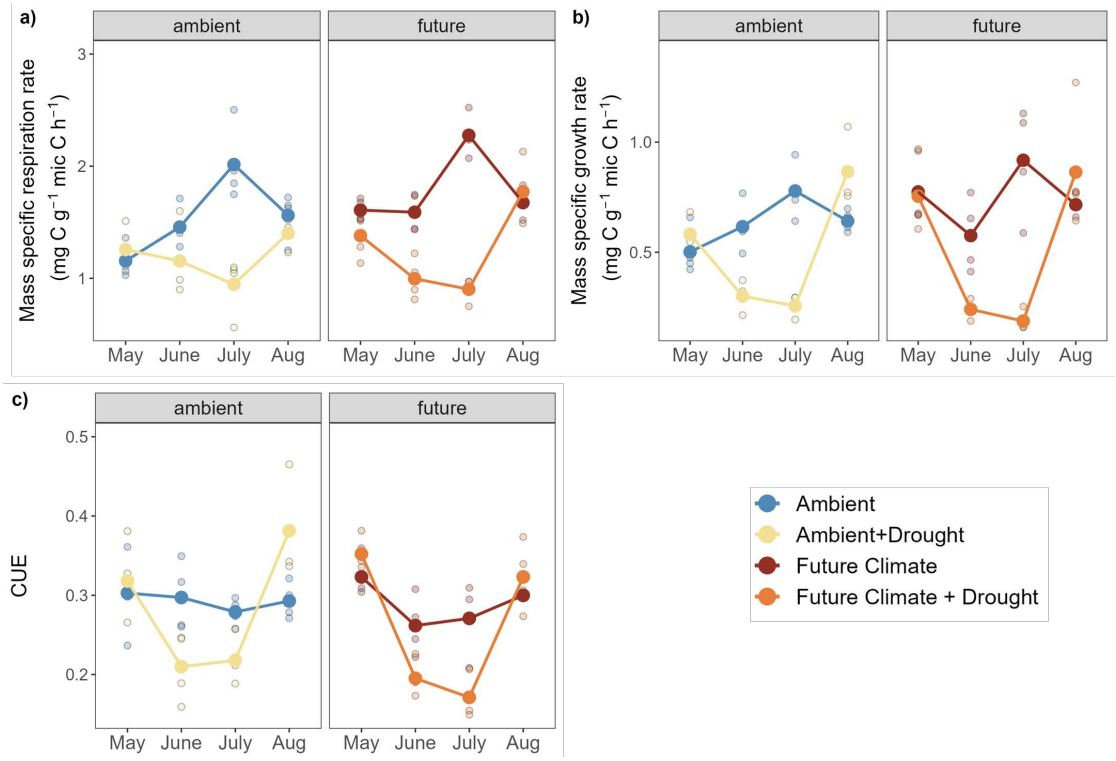

Figure 5: Physiological parameters of soil microbial community, calculated as milligrams of carbon produced in relation to grams of microbial biomass carbon and hour. Mass specific respiration rate (a), mass specific growth rate (b) and carbon use efficiency (CUE) (c) were measured at 4 time points (May [25.05.]: initial conditions; June [26.06.]: beginning of drought period; July [27.07.]: peak drought; August [01.08.]: rewetting) under 'ambient' and 'future' climate (eT and eCO2) conditions. Each line plot is coloured after the specific treatment, representing the mean at each time point.

Table 2: Effect of future climate (C), drought (D) and their interaction (I) on microbial mass-specific respiration, mass-specific growth and carbon use efficiency (CUE). The p-values were derived from linear mixed effect models for each time point (May [25.05.]: initial conditions; June [26.06.]: beginning of drought period; July [27.07.]: peak drought; August [01.08.]: rewetting). The p-values were adjusted (Adj. p) using "Benjamin-Hochberg" method. Significant p-values (<0.05) are represented in bold. See full report in Table 9.

		May	June	July	August
Respiration	*C*	**0.0082**	0.9099	0.9347	0.1520
	D	0.4543	**0.003**	**<0.0001**	0.7168
	I	0.0895	0.2817	0.3501	0.4520
Growth	*C*	**0.0072**	0.4906	0.4503	0.6321
	D	0.6291	**0.0001**	**<0.0001**	0.2101
	I	0.5842	0.8617	0.0839	0.7285
CUE	*C*	0.3683	0.2723	0.0825	0.5482
	D	0.3683	**0.0029**	**0.0012**	0.0845
	I	0.7316	0.5912	0.2722	0.3115

3.3 Microbial community composition

To assess differences in microbial community composition we performed a principal component analysis (PCA) and evaluated differences by a PERMANOVA, using both total abundances and mass-specific growth rates. Additionally, we quantified mass-specific growth rates of individual microbial groups (Figure 6, Table 3).

The composition of the active community was influenced by future climate, drought, and their interaction (Table 3). Future climate changed the composition in May, June, and July, with the greatest impact in May (PERMANOVA: R^2 = 0.22). Drought had an even stronger impact shaping the active community

composition in June, July and even after rewetting in August. The greatest drought influence occurred in July (PERMANOVA: R^2 = 0.64), with additionally a significant interaction of future climate and drought (PERMANOVA: R^2 = 0.08). In May, principal component analysis (PCA) of relative growth rates indicates a separation of the active community composition by climate on PC1 (27.4%) due to a preferential incorporation of ^2H into gram-negative bacteria under ambient climate. Further, the microbial communities growing under ambient climate were predominantly distinct in their composition, while the communities under future climate highly overlapped (Figure 6, top left). In June, the composition of the active community formed individual clusters for all treatments, with drought being the key separator (PC1 61.3%) (Figure 6, top right). At peak drought (July), the growing communities were further divided on PC1 (67.8%) and formed three distinct communities due to the overlap of the communities under ambient - and future climate. Thus, the incorporation of ^2H into fungi was prevalent in the drought-affected plots. On PC2 (20.1%), the interaction of climate and drought formed two distinct compositions, namely by the incorporation of ^2H into gram positive biomarkers under ambient climate and the incorporation into general biomarkers under future climate (Figure 6, bottom left). The drought effect changed the active community even after rewetting (August), resulting in distinct compositions (Figure 6, bottom right).

Total community composition changed in response to both future climate and drought (Figure 12, Table 10). Drought shaped the total community composition during the entire observation period, thus effects of drought from previous years influenced their composition (May, PERMANOVA: R^2 = 0.18). In contrast, future climate only affected the total community composition in May and June. The PCA analysis of the total community composition, indicate a drought induced separation of their composition in May, June, and July with the strongest pattern during peak drought (July). Here drought conditions incorporated into gram-positive

and actinobacteria marker, while non drought affected plots preferentially incorporation into gram-negative and AMF marker. Similar to the active community, the interaction of climate and drought formed two distinct compositions while the communities under ambient - and future climate overlap (Figure 12, bottom left).

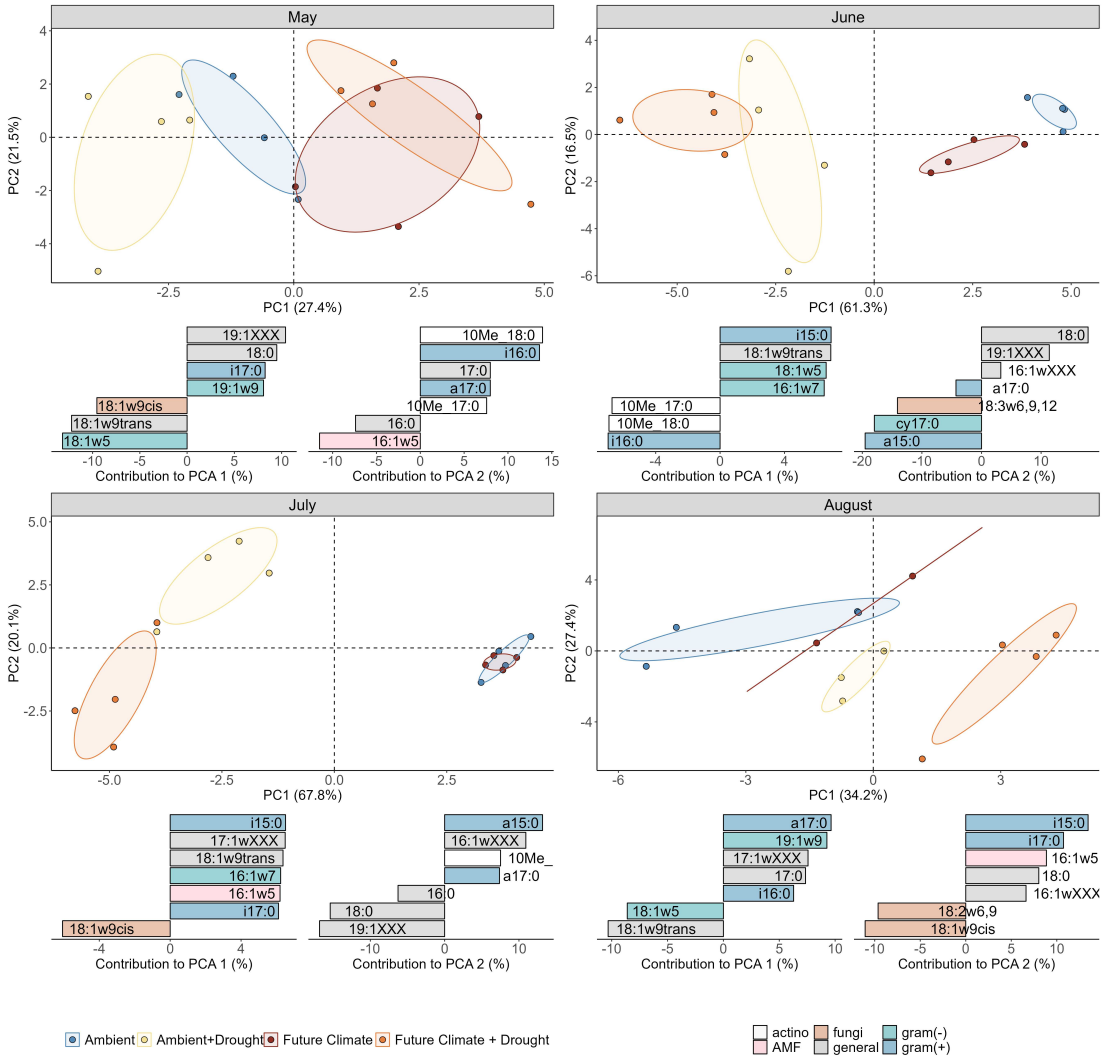

Figure 6: Principal component analysis (PCA) of active microbial community based on ^2H incorporation in PLFA biomarkers. Active community composition coloured by treatment is represented during 4 timepoints (May: initial conditions; June: beginning of drought period; July: peak drought; August: rewetting). The graph below of each PCA plot, show the relative contribution of the individual principal components. This represents the seven most important biomarkers assigned to the microbial groups (gram-positive: blue; gram-negative: light blue; fungi: orange; actinobacteria: white; general markers: grey; arbuscular mycorrhizal fungi: pink).

Table 3: Effect of future climate (C), drought (D) and their interaction (I) on the composition of actively growing PLFA community. We performed a PERMANOVA based on Euclidean distance for each timepoint (May: initial conditions; June: beginning of drought period; July: peak drought; August: rewetting). Significant p-values (<0.05) are represented in bold.

	May		June		July		August	
	R^2	p	R^2	p	R^2	p	R^2	p
C	0.22	**0.0002**	0.09	**0.032**	0.10	**0.01**	0.14	0.051
D	0.09	0.0623	0.53	**0.001**	0.64	**0.001**	0.25	**0.001**
I	0.07	0.1555	0.045	0.155	0.08	**0.015**	0.06	0.404

The mass-specific growth rates of bacteria (sum of gram-positive bacterial marker, gram-negative bacterial marker and actinobacterial marker) were affected by both future climate conditions and drought (Figure 7 a). Specifically, future climate stimulated mass-specific bacterial growth significantly during May, leading to an increase by an average of 47.2%. Drought significantly decreased bacterial growth rates, with a significant interaction between future climate and drought in July (peak drought), as bacterial growth rate decreased by 52% under ambient conditions and by 78% under future climate. After rewetting (August), mass specific bacterial growth recovered and significantly increased compared to control conditions (Figure 7 b). Whereas gram-positive and gram-negative bacterial mass specific growth behaviour match the general bacterial patterns (Figure 7 b), actinobacteria showed resistance to drought, although a significant future climate x drought interaction in July showed a decrease in actinobacteria growth rates under future climate conditions (Figure 7 c). Contrary to bacterial growth patterns, the mass specific fungal growth rates were neither affected by drought nor climate (Figure 7 d). Only the arbuscular mycorrhiza fungi (AMF) biomarker was sensitive to drought and stopped growing (reduction of the growth rate by 99.5%) (Figure 7 e). Drought increased significantly the overall fungal:

bacterial ratio (F:B ratio, excluding AMF) of the microbial community, with a significant interaction between drought and future climate in July where values were more strongly increased under drought conditions (Figure 7 c).

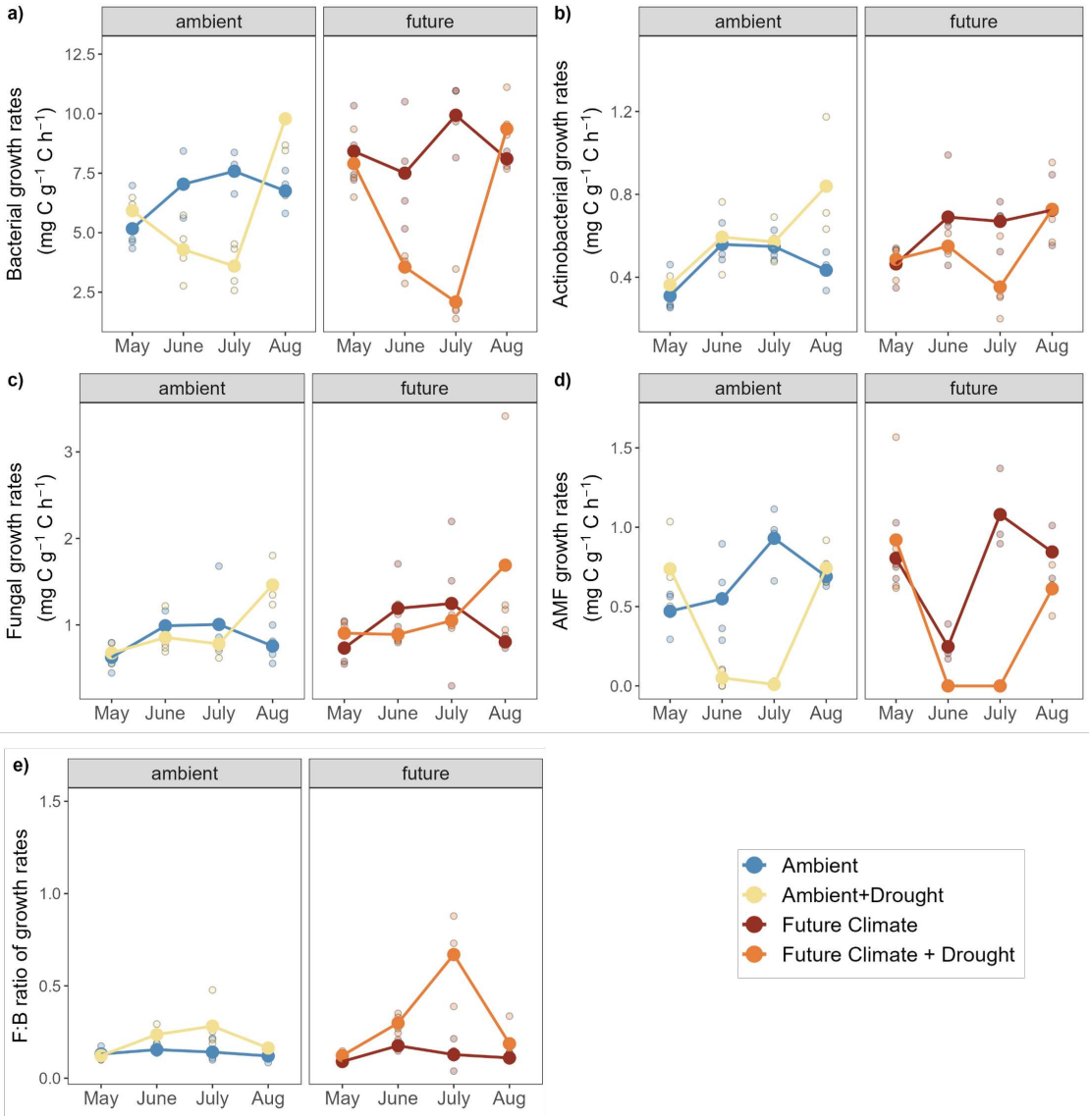

Figure 7: Mass-specific growth rates (PLFA) of soil microbial groups, calculated as milligrams of carbon produced in relation to grams of total carbon of the respective fatty acids and hour. Growth rate of bacterial marker (sum of gram-negative bacterial, gram-positive bacterial and actinobacterial marker) (a), actinobacterial marker (b), fungal marker (c), arbuscular mycorrhiza fungal marker (AMF) (d) and fungal marker to bacterial marker ratio (F:B ratio) (e) were measured at 4 time points (May [25.05.]: initial conditions; June [26.06.]: beginning of drought period; July [27.07.]: peak drought; August [01.08.]: rewetting) under 'ambient' and 'future' climate (eT and eCO2) conditions. Each line plot is coloured after the specific treatment, representing the mean at each time point.

Table 4: Effect of future climate (C), drought (D) and their interaction (I) on mass specific growth rates of bacterial markers, gram-negative bacterial markers, gram-positive bacteria markers, actinobacterial markers, fungal markers, arbuscular mycorrhiza fungal markers (AMF), fungal markers to bacterial markers ratio, and general markers. The p-values were derived from linear mixed effect models for each time point (May [25.05.]: initial conditions; June [26.06.]: beginning of drought period; July [27.07.]: peak drought; August [01.08.]: rewetting). The p-values were adjusted (Adj. p) using "Benjamin-Hochberg" method. Significant p-values (<0.05) are represented in bold. See full report in Table 11 and Table 12.

		May	June	July	August
Bacteria	*C*	**0.0015**	0.8566	0.4231	0.2923
	D	0.8404	**0.0013**	**<0.0001**	**0.0369**
	I	0.3942	0.5705	**0.0034**	0.2923
Actinobacteria	*C*	**0.0064**	0.5383	0.4199	0.2912
	D	0.4519	0.5383	**0.0332**	0.1298
	I	0.6895	0.4618	**0.0243**	0.1352
Fungi	*C*	0.1301	0.4766	0.5150	0.6535
	D	0.2735	0.2055	0.5150	0.0623
	I	0.4740	0.5121	0.9563	0.8874
AMF	*C*	0.1586	**0.0499**	0.9765	0.7718
	D	0.2413	**0.0007**	**<0.0001**	0.5079
	I	0.5825	0.1210	0.1199	0.2019
F/B ratio	*C*	0.1218	0.0631	**0.0142**	0.7378
	D	0.2936	**0.0003**	**0.0004**	0.1181
	I	0.1218	0.3011	**0.0129**	0.7378

3.4 Storage compound production rates

3.4.1 NLFA

At the peak of drought (July), future climate conditions increased mass-specific NLFA production rates of fungi by 60%, while drought increased by 118% on average under future and ambient climate (Figure 8 a). Similarly, gram-negative bacteria showed higher average production due to drought (Figure 8 b) but this result was not significant. When considering the reduction in growth rates during drought and calculating the percentage of NLFA production of gram-negative (Figure 8 d) and fungi (Table 13), as compared to the production of the same PLFA biomarker drought effects became more evident and significant. The NLFA production of AMF decreased significantly during drought (June, July), on average by 85% at the peak of drought. In addition, plots affected by drought in previous years showed a significantly higher NLFA production rate of AMF in May (Figure 8 c).

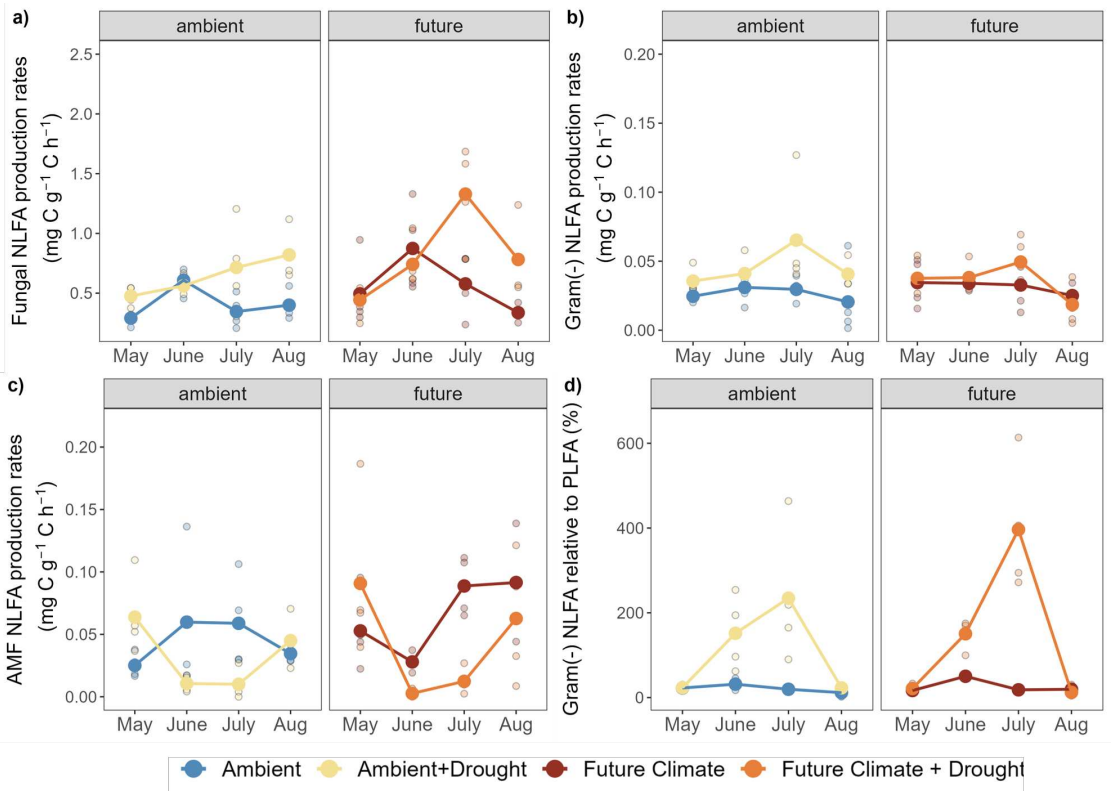

Figure 8: Mass-specific NLFA production rates of soil microbial groups, calculated as milligrams of carbon produced in relation to grams of total carbon of the respective fatty acids and hour. NLFA production rates of fungi (a), gram-negative bacteria (b) and arbuscular mycorrhiza fungi (AMF) (c) and the relative NLFA production rate to PLFA production rate of gram-negative bacteria were measured at 4 time points (May [25.05.]: initial conditions; June [26.06.]: beginning of drought period; July [27.07.]: peak drought; August [01.08.]: rewetting) under 'ambient' and 'future' climate (eT and eCO2) conditions. Each line plot is coloured after the specific treatment, representing the mean at each time point.

Table 5: Effect of future climate (C), drought (D) and their interaction (I) on mass-specific NLFA production rates of fungal markers, fungal markers relative to growth (PLFA), arbuscular mycorrhiza fungal markers (AMF), gram-negative bacterial markers, gram-negative bacterial markers relative to growth (PLFA), and general markers. The p-values were derived from linear mixed effect models for each time point (May [25.05.]: initial conditions; June [26.06.]: beginning of drought period; July [27.07.]: peak drought; August [01.08.]: rewetting). The p-values were adjusted (Adj. p) using "Benjamin-Hochberg" method. Significant p-values (<0.05) are represented in bold. See full report in Table 13.

		May	June	July	August
Fungi	*C*	0.3615	0.1221	**0.0265**	0.923
	D	0.279	0.6545	**0.0079**	**0.0218**
	I	0.279	0.8662	0.2486	0.9292
Gram negative bacteria	*C*	0.4341	0.9966	0.6877	0.4689
	D	0.4341	0.3788	0.0564	0.4689
	I	0.5034	0.7692	0.6877	0.4689
AMF	*C*	0.1365	0.0989	0.2388	0.6199
	D	**0.0417**	**0.0024**	**0.0002**	0.7109
	I	0.4622	0.94	0.5214	0.6199
Gram negative bacteria (relative to growth)	*C*	0.4763	0.1903	0.1745	0.7535
	D	0.54	**<0.0001**	**<0.0001**	0. 7535
	I	0.5498	0.3309	0.155	0.2713

3.4.2 PHB

The mass specific PHB production was stable during the drought period, while the future climate decreased PHB production in June (Figure 9 a). Considering the reduction of the active microbial community during drought, the calculated relative bacterial PHB production increased in June and July (Figure 9 b).

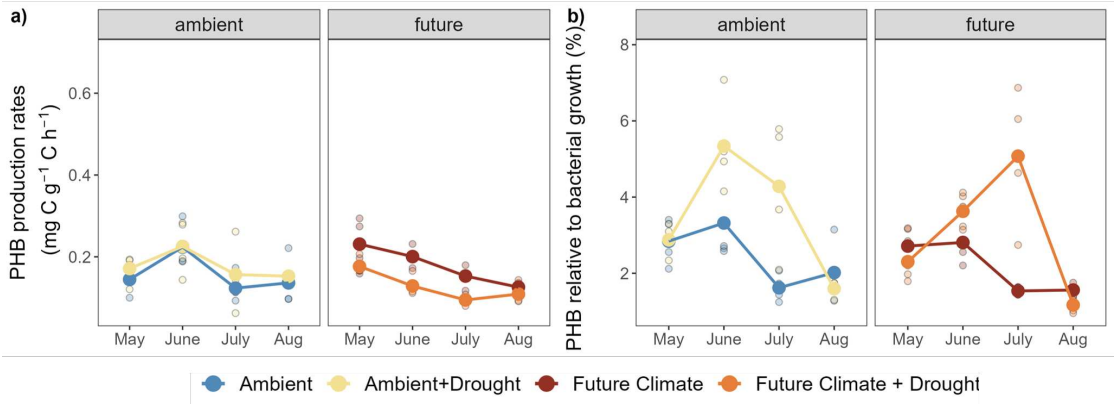

Figure 9: Mass-specific PHB production rates of bacteria, calculated as milligrams of carbon produced in relation to grams of total carbon of the respective fatty acids and hour. PHB production rates of a) bacterial markers and b) the relative bacterial PHB production rate relative to bacterial growth rate were measured at 4 time points (May [25.05.]: initial conditions; June [26.06.]: beginning of drought period; July [27.07.]: peak drought; August [01.08.]: rewetting) under 'ambient' and 'future' climate (eT and eCO2) conditions. Each line plot is coloured after the specific treatment, representing the mean at each time point.

Table 6: Effect of future climate (C), drought (D) and their interaction (I) on mass-specific PHB production rates of bacterial markers and bacterial markers relative to growth (PLFA). The p-values were derived from linear mixed effect models for each time point (May [25.05.]: initial conditions; June [26.06.]: beginning of drought period; July [27.07.]: peak drought; August [01.08.]: rewetting). The p-values were adjusted (Adj. p) using "Benjamin-Hochberg" method. Significant p-values (<0.05) are represented in bold. See full report in Table 14.

		May	June	July	August
PHB	*C*	0.0918	**0.04584**	0.5658	0.3856
	D	0.5119	0.1526	0.5658	0.8505
	I	0.095	0.1526	0.1574	0.3954
PHB relative to growth	*C*	0.4059	0.0796	0.6558	0.1745
	D	0.4851	**0.0168**	**<0.0001**	0.2556
	I	0.4851	0.3498	0.6558	0.9611

4 Discussion

Microbes take up organic carbon and allocate it to various processes, the most prominent of which include cell division (i.e., growth in the strictest sense), energy production (respiration), and the synthesis of storage compounds and osmolytes. Despite the critical role these microbial processes play in ecosystem carbon cycling, our understanding of how they will be affected by future climate conditions remains limited. Most studies to date have focused on the single effects of climate change, such as warming [3, 79], elevated CO_2 [1, 26], or increased drought intensity [63]. However, these factors rarely occur in isolation and multifactorial field experiments are rare [60]. In this study, we quantified in a field experiment the effects of a simulated two-month drought period and future climate conditions (i.e., elevated temperatures of + 3 $^{\circ}\mathrm{C}$ above ambient, and elevated atmospheric CO_2 of + 300 ppm above ambient) on a submontane grassland. Microbial responses were quantified by simultaneously analysing soil microbial growth (PLFA) and the synthesis of storage compounds (NLFA, PHB) using a novel approach of PLFA stable isotope probing with Deuterium-enriched water. We show that drought affected soil community growth and activity, although within microbial groups great differences occurred. While bacterial C allocation was altered in response to drought, fungi appear resistant. Future climate (elevated CO_2 and warming) in our study seems to enhance microbial response the drought affects.

4.1 Contrasting responses of bacteria and fungi to drought

In our experiment, drought significantly impacted microbial activity (i.e., respiration) and overall community growth rate. The onset of drought caused a decline in soil water content (SWC) (Figure 11 a), which in turn altered microbial living conditions. The decline in microbial activity (July reduction 53%, Figure 5 a) indicates that microbial metabolic processes were hampered, likely due to limited water availability affecting cellular functions and substrate accessibility. Furthermore, the substantial reduction in overall community growth (July reduction by 67%, Figure 5 b) indicate not only less active microbes but also significant challenges in reproduction and maintaining biomass. As soil dry, less water-filled soil pores remain, reducing osmotic potential. Consequently, microbes expose to various stress factors, including direct effects (e.g., new equilibration to their environmental conditions or accumulation of solutes to remain hydrated) or indirect effects on soil processes (e.g., alteration of resource supply) [63]. Several mechanisms could explain the concurrent decline in growth rates and activity. For instance, the decrease might indicate a general slowdown of the cell division rate in response to resource shortage, a lower biomass due to higher mortality compared to the growth rate, C reallocation towards storage products or other drought adaptation strategies including dormancy [31] or osmolyte production [63]. Given that the reduction in microbial growth rates was higher compared to their reductions in respiration activity, we suggest that a substantial part of microbes was dormant or shifted their C allocation during drought conditions rather than merely experiencing increased mortality. Moreover, after soil was rewet (August), activity and growth rates returned to previous levels, indicating high resilience after drought events and supporting the notion of physiological adjustments during drought. Consequently, drought has the potential to alter the

soil carbon balance by reducing microbial growth and leading to a smaller and less active microbial community.

In our study, the Carbon Use Efficiency (CUE), which reflects the partitioning of anabolic and catabolic processes in microbes [74], decreased in response to drought, indicating a more significant reduction in growth than in respiration (Figure 5 c). This is consistent with general considerations of Manzoni et al. (2012), which have predicted that CUE would decline in response to warming and decrease to nutrient availability. Similarly, drought forces microbes into unfavourable environmental conditions, enhancing their maintenance costs thus increase their respiratory activity compared to biomass growth [3]. If more carbon is allocated to respiration rather than growth, more carbon can be lost to the atmosphere. However, the typical calculation of CUE overlooks the fact that microorganisms can allocate carbon to storage compounds, which may contribute to total biomass [41], thus interpreting CUE with caution.

To get a comprehensive picture of bacterial growth strategies during drought, we analysed bacterial cell division (PLFAs) and storage compound production (PHB synthesis) by the same ^{2}H-vapour labelling approach. We found, drought strongly reduced bacterial growth rates (Figure 7 a). These findings are consistent with previous studies by Canarini et al. (2023) and Metze et al. (2024), which also observed reduced bacterial growth in response to drought at the same study site. Lower individual growth rates have been suggested to be a survival strategy where bacteria decrease energy consumption and prevent water loss due to an increased accumulation of osmolytes to resist drought [85]. However, Metze et al. (2024) have shown that a large part of bacteria stopped growing, while only fewer taxa dominated the active community. With this, the active bacterial community might occur smaller and less diverse during drought.

Within the bacterial community, we found bacterial growth reductions varied in degree, indicating different sensitivities to drought across bacterial groups.

Gram-positive bacteria exhibited less pronounced growth reductions during drought (-43%) compared to gram-negative bacteria (-70%) (Figure 13 b c). The higher resistance of gram-positive bacteria can be attributed to their advanced osmoregulatory function and a strong peptidoglycan cell wall layer [40, 62]. Within the gram-positive bacteria, specifically the growth rates of actinobacteria were remarkable resistant, indicating a higher drought tolerance. The enrichment of actinobacteria under drought has been previously reported in soils [25, 45, 50], and they are known to be highly tolerant of life in arid environments [73]. This resilience might be attributable to certain taxa within phylum actinobacteria, such as the genus streptomyces, which is known to form spores – as a significant advantage under severe stress conditions [50].

In our experiment, we observed a clear contrast between the bacterial growth rate and the synthesis of polyhydroxybutyrate (PHB), a bacterial storage compound, under drought conditions. While the bacterial growth rate decreased, PHB synthesis either remained constant or increased when comparing the storage synthesis rate with the bacterial growth rate (Figure 9). This finding indicates that under drought conditions, the bacteria use carbon primarily for the synthesis of storage compounds rather than for growth. This aligns with Butler et al. (2023), who found that soil fertility significantly influences microbial carbon storage, with higher allocations to storage compounds in comparatively infertile soils. Given that soil microbes are predominantly carbon-limited [71], and access to resources are restricted during drought, the enhanced accumulation of carbon-rich storage compounds represent an important energy source. Moreover, to cope with temporal variability of environmental conditions, microbes can reduce their metabolic activity by entering dormancy [44]. Dormancy is a reversible state which can enhance microbial resistance and thereby maintaining high levels of microbial diversity [31]. However, entering a physiological state of dormancy increases their energy demand, requiring microbes to invest in dormancy [63]. The degradation of accumulated carbon storage compounds can promote the

transition into or out of dormancy, indicating a shift in resource allocation under drought that prioritizes storage over cell division when resources become scarce, or conditions are unfavourable. This is representing a reserve storage strategy which involves accumulating carbon during periods of limited resource availability, which comes at the expense of other metabolic functions such as reproduction. Bacterial upregulation of PHA/TAG synthesis as response to C-limited conditions has been already reported [11, 42, 57] and in addition many bacterial species are known to increase PHA accumulation as response to osmotic stress [46]. Our used approach, based on water labelling and without adding additional carbon, provides empirical evidence for a reduction in growth accompanied by an increase in carbon-rich intracellular storage compounds under drought conditions. Although there is a plethora of literature on the reduction of bacterial growth rates due to drought, information on how drought affects storage synthesis is limited, particularly regarding group-specific differences within bacteria. To better understand physiological and resource allocation changes in response to drought, it is crucial to investigate storage compound production at the group-specific level.

In addition to bacterial growth strategies, we investigated fungal growth strategies during drought by analysing cell division (PLFAs) and storage compound production (NLFAs) using the ^{2}H-vapour labelling approach. Unlike bacterial growth rates, which declined under drought conditions, fungal growth rates remained unaffected. This observation suggests that fungi possess a higher drought tolerance compared to bacteria. The increased resistance of fungi can be attributed to their hyphal structure, which allows them to access and utilize water from deeper soil layers, even when soil moisture levels are extremely low and diffusivity is limited in the topsoil [62, 63]. Despite their greater drought tolerance, as indicated by consistent growth rates, fungi also enhanced the accumulation of storage compounds (Figure 8 a) as soil moisture decreased. This behaviour

indicates a physiological response where carbon is allocated to storage rather than growth. Previous research has shown that spores of arbuscular mycorrhizal fungi contain more neutral lipid fatty acids (NLFAs) than phospholipid fatty acids (PLFAs) [53], suggesting that the increase in fungal NLFAs might be correlated with an increase in spore formation. The increase in spore formation of fungi during drought provides several advantages that enhance their drought resistance. Firstly, spores act as an insurance against future stresses, remaining dormant until conditions improve [21]. This dormancy ensures fungi can survive prolonged drought periods. Additionally, spores can disperse over large distances, allowing fungi to colonize new areas with more favourable conditions. Furthermore, the degradation of storage compounds during drought provides a competitive advantage. These compounds can support rapid reproduction when conditions become favourable again or when predation risk is low [42]. This shows that fungi not only tolerate drought better due to their filamentous body structure but also strategically allocate resources to enhance their resilience and competitive advantage during and after drought conditions.

In our study, arbuscular mycorrhiza fungi (AMF), which live in symbiosis with vascular plants and exchange nutrients and water in return for plant carbon [69], were very drought sensitive. They significantly reduced their growth rate (Figure 7 d) and their synthesis of storage compounds (Figure 8 c), indicating reduced or absent spore formation and hyphal growth. This was unexpected, as it was previously demonstrated that AMF can acquire essential nutrients and water by extending their hyphae during drought conditions, facilitated by minor physiological adjustments [29]. Our method for quantifying AMF growth rates and storage synthesis involved the removal of host plants, which likely disrupted the AMF symbiosis. However, we found that AMF grow under ambient conditions even when separated from their hosts, and therefore our results suggest that AMF already had no access to plant carbon prior to the experiment. Previous studies

have already shown similar findings of decreasing AMF biomass in response to drought [14, 59]. Despite the high growth reductions during drought, alterations in AMF storage synthesis were already evident in the drought plots even before the onset of drought. Their NLFA production rate was slightly enhanced, possibly a legacy of the droughts of previous years. There is increasing evidence of possible legacy effects after drought [14, 32]. Nevertheless, in our study, after this year's drought event and subsequent rewetting of soil (August), the differences disappeared. Moreover, the use of PLFA 16:1ω5 to quantify AMF biomass is not exclusively indicative of arbuscular mycorrhiza, as this fatty acid is also found in bacterial taxa [54]. Consequently, it is unclear to what extent the biomass estimated via PLFA 16:1ω5 originates from fungi and which part is attributed to bacteria. However, the fact remains, that a legacy effect of previous years was visible already before the onset of new drought.

Altogether, we observed drought significantly affects soil microbial resource allocation (Figure 7), leading to shifts in composition of the active community (Figure 6). The active community exhibited a higher contribution of fungi compared to bacteria (Figure 7 e). Additionally, within the bacteria the abundance of gram-positive bacteria increased compared to gram-negative bacteria, along with more active actinobacteria.

4.2 Microbial responses to drought under future climate conditions

In our experiment, we also examined the effects of drought on microbial communities within the context of simulated future climate conditions (+3°C, +300 ppm). We found, future climate conditions at ambient precipitation levels did not affect SWC, whereas drought-induced decline in SWC were significantly more

pronounced under future climate conditions (Figure 11 a). Rising temperatures can increase evapotranspiration, which reduces soil moisture, while elevated CO_2 levels can enhance soil moisture by decreasing stomatal conductance and thereby lowering evapotranspiration [1, 86]. Previous studies suggest that plant carbon inputs due to elevated CO_2 often have a dominant effect on microbial activity compared to temperature effects [19, 20, 70]. However, in our study, the combined effects of drought and future climate conditions led to an even greater reduction in SWC, likely due to enhanced evaporation, which could intensify the drought effects on soil microbes. This illustrates the complexity of predicting the interactive impacts of elevated CO_2 and temperature on soil microbial communities, as it heavily depends on factors like soil type, plant species composition, and local climate conditions.

Under future climate conditions at ambient precipitation levels, bacterial growth rates and activity (i.e., respiration) were positively stimulated, while their storage compound synthesis remained unchanged (Figure 7 a, Figure 9). The stimulation is likely due to the direct effects of warming on soil microbial decomposition and temperature-sensitive processes (Allison et al., 2010). Additionally, elevated atmospheric CO_2 levels can enhance plant productivity and rhizodeposition, leading to increased belowground carbon allocation [1]. Interestingly, while bacterial growth benefited from these changes, fungal growth remained unaffected. The increase in bacterial growth rates under future climate conditions led to a higher number of bacteria in the active community, which may have contributed to the observed community shift (Figure 6). He et al. (2010) found that elevated CO_2 led to an increase in bacterial biomass but had no effect on fungal biomass. They also observed an increase in genes associated with the degradation of labile carbon, suggesting an increase in the availability of labile carbon. This could be due to a change in microbial lifestyle from oligotrophic to copiotrophic. Fungi are better able to decompose complex organic material and can utilise a wider range

of carbon sources, while bacteria prefer simpler carbon compounds. In addition, the filamentous growth form of fungi provides better access to carbon, potentially making them less constrained by carbon availability compared to bacteria.

Considering the combined effect of future climate and drought, we found that bacterial growth rates were altered, while their synthesis of storage compounds remained unchanged. As the bacteria are rather drought-sensitive, the intensified decline in soil water content likely intensified their resource limitations, leading to reduced growth rates (Figure 7 a). Actinobacteria which were relatively drought-resistant under ambient climate conditions, experienced a strong decrease in growth rates under future climate conditions (Figure 7 b). This significant reduction in growth was observed only during periods of intense drought (e.g., July), suggesting that the intensity of drought modifies how future climate conditions impact bacterial growth. Our results do not corroborate the findings of Metze et al. (2024) at the same experiment, who observed that future climate conditions mitigate effects of drought on bacterial growth. They suggested that this mitigation was due to either a pre-exposure of microorganisms to higher temperatures (and thus in part lower water availability), leading to more drought-tolerant taxa, or to a higher carbon input from plants. In our study, however, microbes that had been pre-exposed to future climate conditions for several years and did not become more drought tolerant. It is important to note that field drought experiments lead to different stresses in different years, depending on field temperatures and relative humidity. Fungal growth rates, similar to their response under single drought conditions, remained unaffected by the additional future climate conditions. Despite their notable resilience under both drought and future climate scenarios, fungi increased their accumulation of storage compounds during peak drought (Figure 8 a). This increase underscores their higher resistance during unfavourable conditions. The further decline in bacterial growth compared to fungal growth during the drought and future climate suggests that

future climate conditions will become a more important factor in the composition of active communities as the duration of the drought increases.

In summary, our study demonstrates that both drought and future climate conditions significantly impact soil microbial communities. Drought affected microbial growth, activity, and carbon utilization. The extend to which microbes were affected differed for specific microbial groups. Bacterial growth rates were reduced, except for actinobacteria, while synthesis of storage compounds (PHB) increased in response to drought. In contrast, fungal growth rates remained constant, accompanied by a concomitant increase in their synthesis of storage compounds (NLFA). Under the combined effects of drought and future climate conditions, bacterial growth rates were further reduced, while fungi showed remarkable resistance. This highlights the importance of storage compounds as adaptations for microbes to sustain unfavourable conditions. The physiological responses of microbes and their carbon use strategies may have profound implications for the carbon cycle and the trajectory of future climate change. Understanding these interactions is crucial for predicting and managing the effects of climate change on soil ecosystems and global carbon dynamics.

5 Supplementary Material

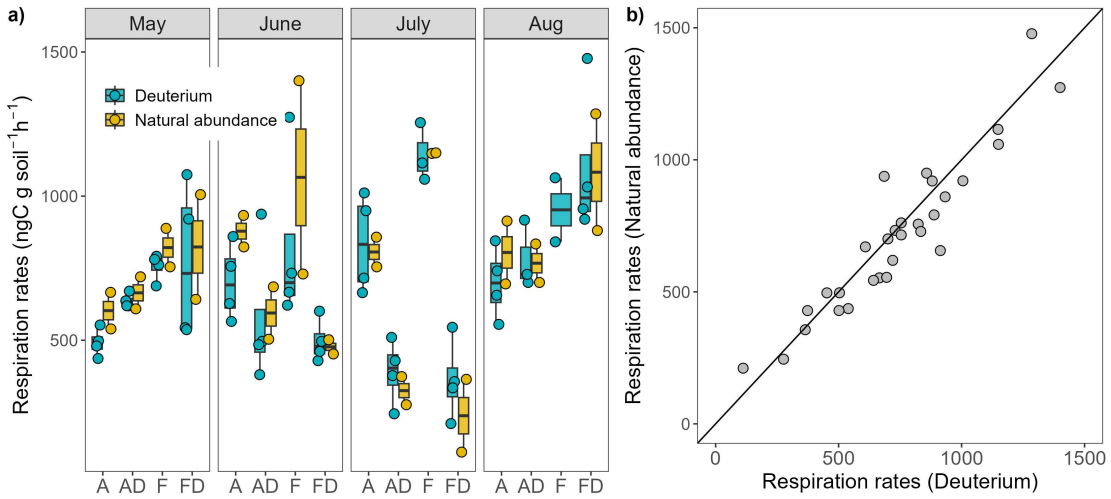

Figure 10: Respiration rates of deuterium incorporated samples [^{2}H labelled] and natural abundance [non labelled]. Month wise comparisons of respiration rates (a) (May [25.05.]: initial conditions; June [26.06.]: beginning of drought period; July [27.07.]: peak drought; August [01.08.]: rewetting) for each treatment (A: Ambient; AD: Ambient + Drought; F: Future climate; FD: Future climate + Drought). Box plot represents range within the samples (Median is represented by box center, box indicate upper and lower quartiles, whiskers the 1.5x interquartile range and separated points the outliers). Correlation plot between deuterium incorporated samples and natural abundance (b).

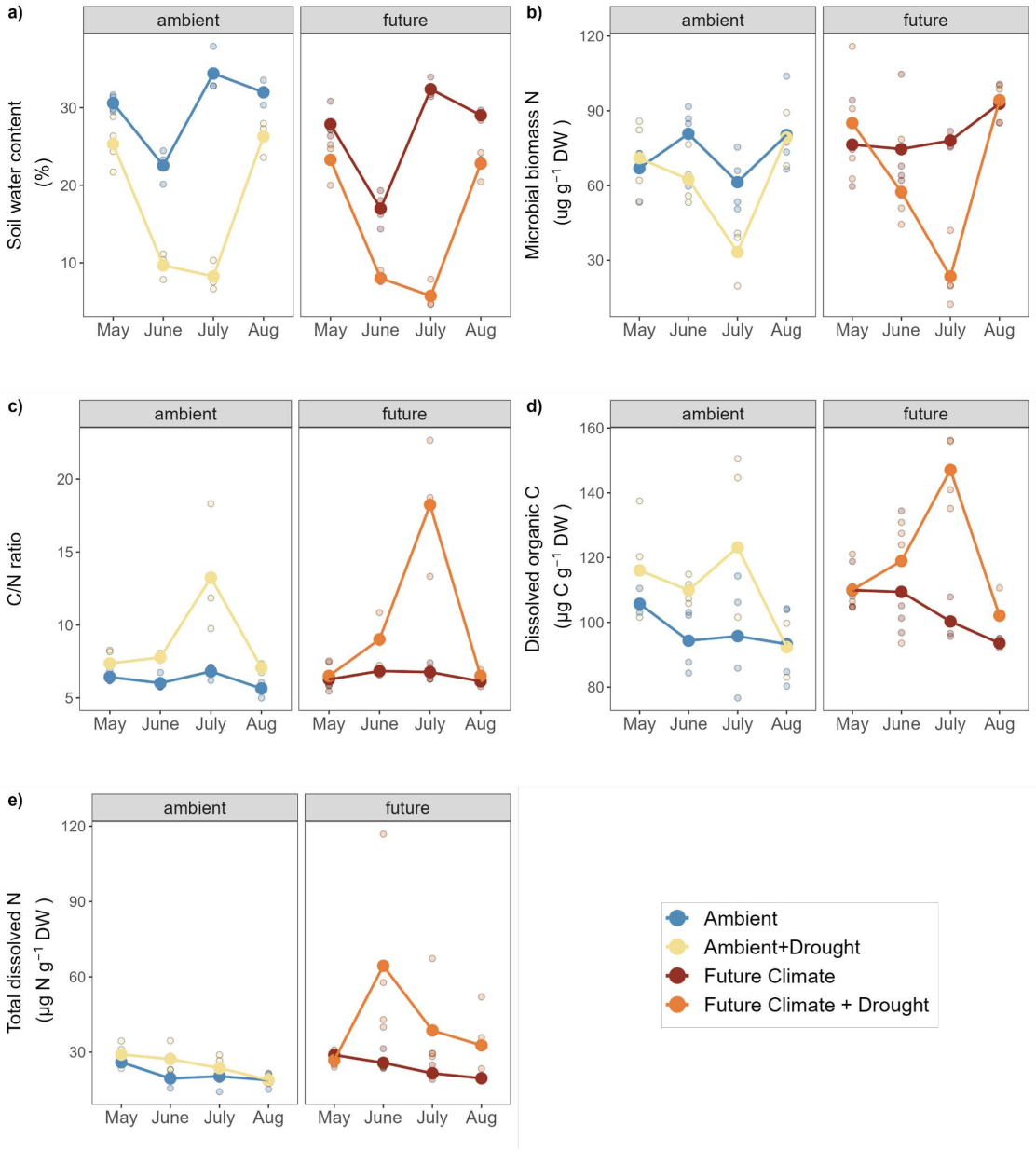

Figure 11: Soil and microbial soil community parameters. Soil water content (%) (a), Microbial biomass nitrogen (MBN) (b), Carbon to nitrogen ratio (c), Dissolved organic carbon (d) and Total dissolved nitrogen (e) were measured at 4 time points (May [25.05.]: initial conditions; June [26.06.]: beginning of drought period; July [27.07.]: peak drought; August [01.08.]: rewetting) under 'ambient' and 'future' climate (eT and eCO2) conditions. Each line plot is coloured after the specific treatment, representing the mean at each time point.

Table 7: Effect of future climate (C), drought (D) and their interaction (I) on soil water content (SWC), total C produced, microbial biomass nitrogen, carbon to nitrogen (C/N) ratio, dissolved organic carbon (DOC) and total dissolved organic nitrogen (TDN). The p-values were derived from linear mixed effect models for each time point (May [25.05.]: initial conditions; June [26.06.]: beginning of drought period; July [27.07.]: peak drought; August [01.08.]: rewetting). The p-values were adjusted (Adj. p) using "Benjamin-Hochberg" method. Significant p-values (<0.05) are represented in bold.

		May			June			July			August		
		F	p	Adj. p	F	p	Adj. p	F	p	Adj. p	F	p	Adj. p
SWC	*C*	4.536	0.055	0.073	19.724	**0.001**	**0.001**	7.476	**0.018**	**0.024**	24.938	**0.001**	**0.001**
	D	19.468	**0.001**	**0.002**	181.868	**<0.0001**	**<0.0001**	405.797	**<0.0001**	**<0.0001**	37.994	**0.000**	**0.000**
	I	0.095	0.763	0.763	5.795	**0.033**	**0.033**	3.936	0.071	0.071	0.074	0.791	0.791
C produced	*C*	6.737	**0.023**	**0.047**	0.387	0.546	0.726	2.191	0.165	0.165	2.116	0.180	0.240
	D	1.895	0.194	0.258	19.479	**0.001**	**0.002**	46.034	**0.000**	**0.000**	3.824	0.082	0.164
	I	0.033	0.860	0.860	0.129	0.726	0.726	4.416	0.057	0.077	0.127	0.730	0.730
MBN	*C*	2.042	0.179	0.357	0.533	0.479	0.639	0.486	0.499	0.499	4.369	0.066	0.132
	D	0.593	0.456	0.608	5.345	**0.039**	0.079	68.570	**0.000**	**<0.0001**	0.000	0.995	0.995
	I	0.079	0.784	0.784	0.005	0.943	0.943	7.037	**0.021**	**0.028**	0.030	0.866	0.995
C/N ratio	*C*	1.764	0.209	0.278	8.110	**0.015**	**0.020**	3.199	0.099	0.099	0.402	0.542	0.542
	D	2.299	0.155	0.278	30.914	**0.000**	**0.000**	81.021	**<0.0001**	**<0.0001**	19.269	**0.002**	**0.003**
	I	0.826	0.381	0.381	0.005	0.944	0.944	3.525	0.085	0.099	5.661	**0.041**	0.055
DOC	*C*	0.033	0.859	0.859	3.344	0.092	0.123	2.639	0.130	0.174	1.582	0.240	0.480
	D	1.146	0.305	0.422	3.648	0.080	0.123	16.089	**0.002**	**0.003**	0.378	0.554	0.554
	I	1.094	0.316	0.422	0.209	0.655	0.655	0.785	0.393	0.393	0.811	0.391	0.522
TDN	*C*	0.049	0.829	0.829	5.632	**0.035**	**0.047**	3.527	0.085	0.113	4.890	0.054	0.109
	D	0.114	0.741	0.829	6.434	**0.026**	**0.047**	6.147	**0.029**	0.058	1.595	0.238	0.238
	I	2.997	0.109	0.218	2.865	0.116	0.116	1.801	0.205	0.204	1.814	0.211	0.238

Table 8: Effect of future climate (C), drought (D) and their interaction (I) on microbial biomass carbon (MBC), phospholipid fatty acids (PLFA), neutral lipid fatty acids (NLFAs) and polyhydroxybutyrate (PHB). The p-values were derived from linear mixed effect models for each time point (May [25.05.]: initial conditions; June [26.06.]: beginning of drought period; July [27.07.]: peak drought; August [01.08.]: rewetting). The p-values were adjusted (Adj. p) using "Benjamin-Hochberg" method. Significant p-values (<0.05) are represented in bold.

		May			June			July			August		
		F	p	Adj. p	F	p	Adj. p	F	p	Adj. p	F	p	Adj. p
MBC	*C*	1.120	0.310	0.413	0.291	0.600	0.977	1.385	0.262	0.262	9.517	**0.013**	**0.026**
	D	5.100	**0.043**	0.087	0.001	0.977	0.977	3.083	0.105	0.147	5.803	**0.039**	0.052
	I	0.120	0.738	0.738	0.015	0.904	0.977	2.975	0.110	0.147	0.829	0.386	0.386
PLFA	*C*	1.227	0.290	0.439	0.102	0.755	0.910	1.306	0.276	0.367	0.350	0.569	0.569
	D	1.036	0.329	0.439	0.013	0.910	0.910	0.687	0.423	0.423	1.337	0.277	0.370
	I	0.136	0.718	0.718	0.165	0.692	0.910	2.592	0.133	0.267	3.129	0.111	0.221
NLFA	*C*	14.923	**0.002**	**0.005**	1.652	0.223	0.297	2.048	0.178	0.237	7.715	**0.022**	**0.029**
	D	2.066	0.176	0.176	3.435	0.089	0.177	2.446	0.144	0.237	7.907	**0.020**	**0.029**
	I	3.636	0.081	0.108	0.005	0.943	0.943	0.047	0.833	0.832	0.627	0.449	0.449
PHB	*C*	5.095	**0.043**	0.087	3.828	0.074	0.148	4.663	0.052	0.104	1.051	0.332	0.664
	D	0.597	0.455	0.605	0.165	0.691	0.691	0.395	0.542	0.703	0.182	0.680	0.906
	I	0.281	0.605	0.605	0.173	0.685	0.691	0.152	0.703	0.703	0.014	0.909	0.909

Table 9: Effect of future climate (C), drought (D) and their interaction (I) on microbial mass-specific respiration, mass-specific growth and carbon use efficiency (CUE). The p-values were derived from linear mixed effect models for each time point (May [25.05.]: initial conditions; June [26.06.]: beginning of drought period; July [27.07.]: peak drought; August [01.08.]: rewetting). The p-values were adjusted (Adj. p) using "Benjamin-Hochberg" method. Significant p-values (<0.05) are represented in bold.

		May			June			July			August		
		F	p	Adj. p	F	p	Adj. p	F	p	Adj. p	F	p	Adj. p
Respiration	*C*	12.475	**0.004**	**0.008**	0.013	0.910	0.910	0.007	0.935	0.935	4.019	0.076	0.152
	D	0.598	0.454	0.454	16.628	**0.002**	**0.003**	88.553	**<0.0001**	**<0.0001**	0.140	0.717	0.717
	I	4.051	0.067	0.090	1.744	0.211	0.282	1.394	0.263	0.350	1.020	0.339	0.452
Growth	*C*	13.004	**0.004**	**0.007**	0.875	0.368	0.491	0.609	0.450	0.450	0.640	0.444	0.632
	D	0.246	0.629	0.629	36.340	**0.000**	**0.000**	143.009	**<0.0001**	**<0.0001**	4.033	0.076	0.210
	I	0.643	0.438	0.584	0.032	0.862	0.862	4.202	0.063	0.084	0.326	0.582	0.728
CUE	*C*	1.967	0.186	0.368	1.803	0.204	0.272	4.319	0.062	0.083	0.389	0.548	0.548
	D	1.302	0.276	0.368	16.876	**0.001**	**0.003**	22.461	**0.001**	**0.001**	5.594	**0.042**	0.084
	I	0.123	0.732	0.732	0.304	0.591	0.591	1.336	0.272	0.272	1.631	0.234	0.311

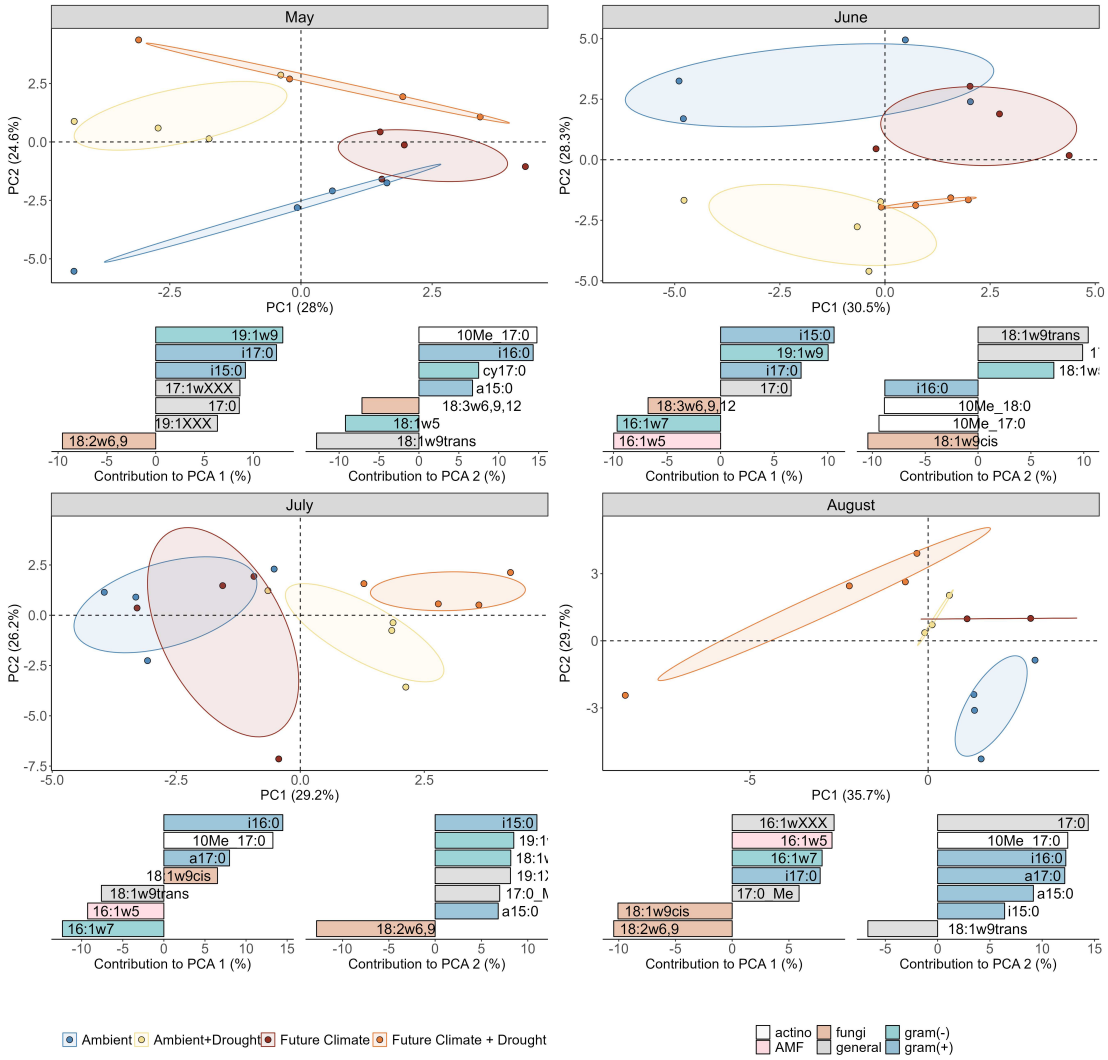

Figure 12: Principal component analysis (PCA) of total microbial community based in ^2H incorporation in PLFA biomarkers. Total community composition coloured by treatment is represented during 4 timepoints (May: initial conditions; June: beginning of drought period; July: peak drought; August: rewetting). The graph below of each PCA plot, show the relative contribution of the individual principal components. This represents the seven most important biomarkers assigned to the microbial groups (gram-positive: blue; gram-negative: light blue; fungi: orange; actinobacteria: white; general markers: grey; arbuscular mycorrhizal fungi: pink).

Table 10: Effect of future climate (C), drought (D) and their interaction (I) on the composition of total PLFA community. We performed a PERMANOVA based on Euclidean distance for each timepoint (May: initial conditions; June: beginning of drought period; July: peak drought; August: rewetting). Significant p-values (<0.05) are represented in bold.

	May		June		July		August	
	R^2	p	R^2	p	R^2	p	R^2	p
C	0.14	**0.008**	0.13	**0.012**	0.09	0.065	0.12	0.075
D	0.19	**0.003**	0.23	**0.001**	0.24	**0.001**	0.25	**0.001**
I	0.03	0.731	0.07	0.197	0.07	0.14	0.09	0.183

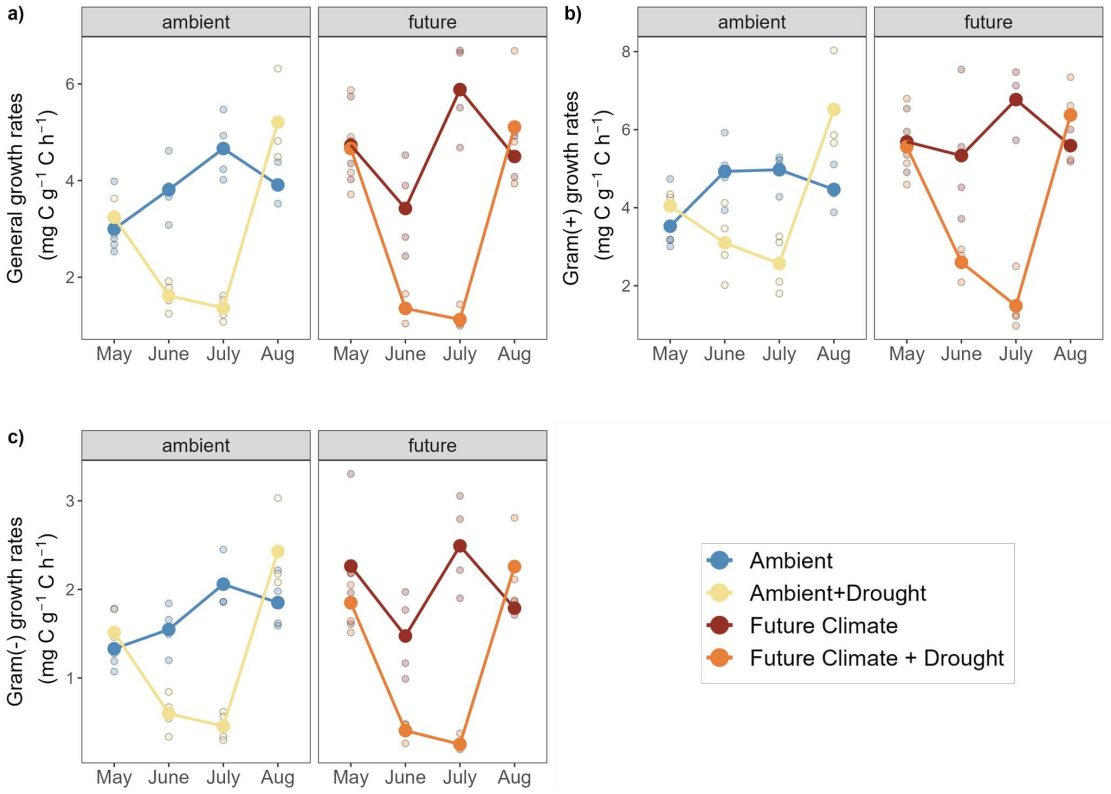

Figure 13: Mass-specific growth rates (PLFA) of soil microbial groups, calculated as milligrams of carbon produced in relation to grams of total carbon of the respective fatty acids and hour. Growth rates of a) general markers, b) gram-positive bacterial markers, c) gram-negative bacteria markers were measured at 4 time points (May [25.05.]: initial conditions; June [26.06.]: beginning of drought period; July [27.07.]: peak drought; August [01.08.]: rewetting) under 'ambient' and 'future' climate (eT and eCO2) conditions. Each line plot is coloured after the specific treatment, representing the mean at each time point.

Table 11: Effect of future climate (C), drought (D) and their interaction (I) on mass specific growth rates of bacterial markersbacterial marker (include marker of gram-negative, gram positive and actinobacteria), gram negative bacterial markers, gram positive bacteria markers, actinobacterial markers and general markers. The p-values were derived from linear mixed effect models for each time point (May [25.05.]: initial conditions; June [26.06.]: beginning of drought period; July [27.07.]: peak drought; August [01.08.]: rewetting). The p-values were adjusted (Adj. p) using “Benjamin-Hochberg” method. Significant p-values (<0.05) are represented in bold.

		May			June			July			August		
		F	p	Adj. p	F	p	Adj. p	F	p	Adj. p	F	p	Adj. p
Bacteria	*C*	20.171	**0.001**	**0.001**	0.034	0.857	0.857	0.688	0.423	0.423	1.357	0.274	0.292
	D	0.042	0.840	0.840	21.039	**0.001**	**0.001**	135.072	**<0.0001**	**<0.0001**	8.237	**0.019**	**0.037**
	I	1.196	0.296	0.394	0.673	0.428	0.570	14.370	**0.003**	**0.003**	1.251	0.292	0.292
Gram negative bacteria	*C*	8.296	**0.014**	**0.028**	2.033	0.179	0.239	2.284	0.157	0.157	0.000	0.990	0.990
	D	0.273	0.611	0.611	54.822	**<0.0001**	**<0.0001**	209.648	**<0.0001**	**<0.0001**	5.945	**0.037**	0.075
	I	1.852	0.199	0.265	0.861	0.372	0.372	8.172	**0.014**	0.157	0.061	0.811	0.990
Gram positive bacteria	*C*	24.867	**0.000**	**0.001**	0.008	0.932	0.932	1.132	0.308	0.308	2.496	0.149	0.198
	D	0.285	0.603	0.603	19.125	**0.001**	**0.002**	131.994	**<0.0001**	**<0.0001**	8.937	**0.015**	**0.030**
	I	0.758	0.401	0.535	0.747	0.404	0.539	18.543	**0.001**	**0.001**	1.568	0.242	0.242
Actinobacteria	*C*	13.475	**0.003**	**0.006**	0.401	0.538	0.538	0.698	0.420	0.420	1.257	0.291	0.291
	D	0.992	0.339	0.452	0.570	0.465	0.538	6.564	**0.025**	**0.033**	4.419	0.065	0.130
	I	0.168	0.689	0.690	1.593	0.231	0.462	8.696	**0.012**	**0.024**	3.329	0.101	0.135
General	*C*	20.114	**0.001**	**0.001**	2.026	0.180	0.240	0.049	0.828	0.828	0.846	0.382	0.502
	D	0.061	0.809	0.809	68.860	**<0.0001**	**<0.0001**	288.033	**<0.0001**	**<0.0001**	4.140	0.072	0.145
	I	0.197	0.665	0.809	0.054	0.820	0.820	6.097	**0.030**	0.039	0.488	0.502	0.502

Table 12: Effect of future climate (C), drought (D) and their interaction (I) on mass specific growth rates of fungal markers, arbuscular mykorrhiza fungal markers (AMF) and fungal markers to bacterial markers ratio. The p-values were derived from linear mixed effect models for each time point (May [25.05.]: initial conditions; June [26.06.]: beginning of drought period; July [27.07.]: peak drought; August [01.08.]: rewetting). The p-values were adjusted (Adj. p) using "Benjamin-Hochberg" method. Significant p-values (<0.05) are represented in bold.

		May			June			July			August		
		F	p	Adj. p	F	p	Adj. p	F	p	Adj. p	F	p	Adj. p
Fungi	*C*	4.124	0.065	0.130	0.916	0.357	0.477	1.180	0.299	0.515	0.901	0.367	0.654
	D	1.795	0.205	0.274	3.120	0.103	0.206	0.809	0.386	0.515	8.853	**0.016**	0.062
	I	0.546	0.474	0.474	0.456	0.512	0.512	0.003	0.956	0.956	0.021	0.887	0.887
AMF	*C*	3.676	0.079	0.159	5.475	**0.037**	**0.050**	0.001	0.977	0.977	0.089	0.772	0.772
	D	2.017	0.181	0.241	24.577	**0.000**	**0.001**	573.126	**<0.0001**	**<0.0001**	0.849	0.381	0.508
	I	0.319	0.582	0.583	2.786	0.121	0.121	3.402	0.090	0.120	3.338	0.101	0.202
F/B ratio	*C*	3.368	0.091	0.122	4.881	**0.047**	0.063	8.220	**0.014**	**0.014**	0.247	0.631	0.738
	D	1.206	0.294	0.294	29.422	**0.000**	**0.000**	27.352	**0.000**	**0.000**	4.667	0.059	0.118
	I	3.603	0.082	0.122	1.168	0.301	0.301	9.449	0.010	0.013	0.119	0.738	0.738

Table 13: Effect of future climate (C), drought (D) and their interaction (I) on mass-specific NLFA production rates of fungal markers, fungal markers relative to growth (PLFA), arbuscular mykorrhiza fungal markers (AMF), gram-negative bacterial markers, gram-negative bacterial markers relative to growth (PLFA), and general markers. The p-values were derived from linear mixed effect models for each time point (May [25.05.]: initial conditions; June [26.06.]: beginning of drought period; July [27.07.]: peak drought; August [01.08.]: rewetting). The p-values were adjusted (Adj. p) using "Benjamin-Hochberg" method. Significant p-values (<0.05) are represented in bold.

		May			June			July			August		
		F	p	Adj. p	F	p	Adj. p	F	p	Adj. p	F	p	Adj. p
Fungi	*C*	0.900	0.362	0.362	4.270	0.061	0.122	7.202	**0.020**	**0.027**	0.167	0.692	0.923
	D	1.761	0.209	0.279	0.505	0.491	0.655	12.638	**0.004**	**0.008**	10.209	**0.011**	**0.022**
	I	2.385	0.148	0.279	0.030	0.866	0.866	1.471	0.249	0.249	0.008	0.929	0.929
Fungi (relative to growth)	*C*	0.006	0.942	0.942	0.490	0.497	0.497	0.713	0.415	0.553	7.335	**0.024**	**0.048**
	D	0.022	0.884	0.942	5.589	**0.036**	**0.048**	53.542	**0.000**	**<0.0001**	2.124	0.179	0.239
	I	5.948	**0.031**	0.062	6.197	**0.028**	**0.048**	0.012	0.914	0.914	0.382	0.552	0.552
AMF	*C*	3.128	0.102	0.137	3.825	0.074	0.099	2.036	0.172	0.239	0.582	0.465	0.620
	D	7.067	**0.021**	**0.042**	17.787	**0.001**	**0.002**	33.754	**0.000**	**0.000**	0.146	0.711	0.711
	I	0.577	0.462	0.462	0.006	0.940	0.940	0.436	0.521	0.521	0.786	0.398	0.620
Gram negative bacteria	*C*	1.051	0.326	0.434	0.000	0.997	0.997	0.211	0.654	0.688	0.597	0.459	0.469
	D	1.494	0.245	0.434	1.936	0.189	0.379	6.218	**0.028**	0.056	0.572	0.469	0.469
	I	0.476	0.503	0.503	0.329	0.577	0.769	0.170	0.688	0.688	1.405	0.266	0.469
Gram negative bacteria (relative to growth)	*C*	1.541	0.238	0.476	2.461	0.143	0.190	2.084	0.175	0.175	0.105	0.753	0.754
	D	0.746	0.405	0.540	39.011	**<0.0001**	**<0.0001**	169.290	**<0.0001**	**<0.0001**	0.313	0.589	0.754
	I	0.379	0.550	0.550	1.027	0.331	0.331	2.866	0.116	0.155	2.686	0.136	0.271
General	*C*	5.031	**0.045**	0.059	0.067	0.800	0.983	0.390	0.544	0.692	0.597	0.459	0.613
	D	7.090	**0.021**	**0.041**	0.000	0.983	0.983	4.860	**0.048**	0.096	6.797	**0.028**	0.057
	I	2.113	0.172	0.172	2.390	0.148	0.296	0.164	0.692	0.692	0.001	0.980	0.980

Table 14: Effect of future climate (C), drought (D) and their interaction (I) on mass-specific PHB production rates of bacterial markers and bacterial markers relative to growth (PLFA). The p-values were derived from linear mixed effect models for each time point (May [25.05.]: initial conditions; June [26.06.]: beginning of drought period; July [27.07.]: peak drought; August [01.08.]: rewetting). The p-values were adjusted (Adj. p) using "Benjamin-Hochberg" method. Significant p-values (<0.05) are represented in bold.

		May			June			July			August		
		F	p	Adj. p	F	p	Adj. p	F	p	Adj. p	F	p	Adj. p
Bacteria	*C*	4.950	**0.046**	0.092	6.798	**0.023**	**0.046**	0.485	0.500	0.566	1.982	0.193	0.386
	D	0.457	0.512	0.512	2.333	0.153	0.153	0.296	0.596	0.566	0.038	0.851	0.851
	I	3.906	0.072	0.095	2.543	0.137	0.153	3.863	0.073	0.157	1.228	0.297	0.395
Bacteria (relative to growth)	*C*	1.814	0.203	0.406	4.682	0.060	0.080	0.210	0.656	0.656	3.681	0.087	0.175
	D	0.519	0.485	0.485	9.030	**0.008**	**0.017**	38.035	**<0.0001**	**<0.0001**	1.992	0.192	0.256
	I	0.730	0.410	0.485	1.204	0.350	0.350	0.457	0.512	0.656	0.003	0.961	0.961

Bibliography

[1] Adair, C. E., Reich, P. B., Trost, J. J., and Hobbie, S. E. (2011). Elevated CO2 stimulates grassland soil respiration by increasing carbon inputs rather than by enhancing soil moisture. *Global Change Biology 17*, ISBN: 1354-1013 Publisher: Wiley Online Library, 3546–3563.

[2] Albi, T., and Serrano, A. (2016). Inorganic polyphosphate in the microbial world. Emerging roles for a multifaceted biopolymer. *World Journal of Microbiology and Biotechnology 32*, ISBN: 0959-3993 Publisher: Springer, 1–12.

[3] Allison, S. D., Wallenstein, M. D., and Bradford, M. A. (2010). Soil-carbon response to warming dependent on microbial physiology. *Nature Geoscience 3*, ISBN: 1752-0894 Publisher: Nature Publishing Group UK London, 336–340.

[4] Alvarez, H., and Steinbüchel, A. (2002). Triacylglycerols in prokaryotic microorganisms. *Applied microbiology and biotechnology 60*, ISBN: 0175-7598 Publisher: Springer, 367–376.

[5] Archer, D., Eby, M., Brovkin, V., Ridgwell, A., Cao, L., Mikolajewicz, U., Caldeira, K., Matsumoto, K., Munhoven, G., and Montenegro, A. (2009). Atmospheric lifetime of fossil fuel carbon dioxide. *Annual review of earth and planetary sciences 37*, ISBN: 0084-6597 Publisher: Annual Reviews, 117–134.

[6] Ayub, N. D., Tribelli, P. M., and López, N. I. (2009). Polyhydroxyalkanoates are essential for maintenance of redox state in the Antarctic bacterium Pseudomonas sp. 14-3 during low temperature adaptation. *Extremophiles 13*, ISBN: 1431-0651 Publisher: Springer, 59–66.

[7] Barnard, R. L., Blazewicz, S. J., and Firestone, M. K. (2020). Rewetting of soil: revisiting the origin of soil CO2 emissions. *Soil Biology and Biochemistry 147*, ISBN: 0038-0717 Publisher: Elsevier, 107819.

[8] Bligh, E. G., and Dyer, W. J. (1959). A rapid method of total lipid extraction and purification. *Canadian journal of biochemistry and physiology 37*, ISBN: 0576-5544 Publisher: NRC Research Press Ottawa, Canada, 911–917.

[9] Borchers, H. W., and Borchers, M. H. W. (2019). Package 'pracma'. *Practical numerical math functions, version 2*.

[10] Brookes, P. C., Landman, A., Pruden, G., and Jenkinson, D. S. (1985). Chloroform fumigation and the release of soil nitrogen: a rapid direct extraction method to measure microbial biomass nitrogen in soil. *Soil biology and biochemistry 17*, ISBN: 0038-0717 Publisher: Elsevier, 837–842.

[11] Butler, O. M., Manzoni, S., and Warren, C. R. (2023). Community composition and physiological plasticity control microbial carbon storage across natural and experimental soil fertility gradients. *The ISME Journal 17*, ISBN: 1751-7362 Publisher: Oxford University Press, 2259–2269.

[12] Canadell, J. G., Monteiro, P. M., Costa, M. H., Cotrim da Cunha, L., Cox, P. M., Eliseev, A. V., Henson, S., Ishii, M., Jaccard, S., and Koven, C., Intergovernmental Panel on Climate Change (IPCC). Global carbon and other biogeochemical cycles and feedbacks In Cambridge University Press: 2023, pp 673–816.

[13] Canarini, A., Fuchslueger, L., Schnecker, J., Metze, D., Nelson, D. B., Kahmen, A., Watzka, M., Pötsch, E. M., Schaumberger, A., and Bahn, M. (2023). Soil fungi remain active and invest in storage compounds during drought independent of future climate conditions. *bioRxiv*, Publisher: Cold Spring Harbor Laboratory, 2023.10. 23.563577.

[14] Canarini, A., Schmidt, H., Fuchslueger, L., Martin, V., Herbold, C. W., Zezula, D., Gündler, P., Hasibeder, R., Jecmenica, M., Bahn, M., and Richter, A. (2021). Ecological memory of recurrent drought modifies soil processes via changes in soil microbial community. *Nature Communications 12*, Publisher: Nature Publishing Group, 5308.

[15] Canarini, A., Wanek, W., Watzka, M., Sandén, T., Spiegel, H., Šantrůček, J., and Schnecker, J. (2020). Quantifying microbial growth and carbon use efficiency in dry soil environments via 18O water vapor equilibration. *Global Change Biology 26*, ISBN: 1354-1013 Publisher: Wiley Online Library, 5333–5341.

[16] Caro, T. A., McFarlin, J., Jech, S., Fierer, N., and Kopf, S. (2023). Hydrogen stable isotope probing of lipids demonstrates slow rates of microbial growth in soil. *Proceedings of the National Academy of Sciences 120*, Publisher: Proceedings of the National Academy of Sciences, DOI: 10.1073/pnas.2211625120.

[17] Chapin III, F. S., Schulze, E. D., and Mooney, H. A. (1990). The ecology and economics of storage in plants. *Annual review of ecology and systematics 21*, ISBN: 0066-4162 Publisher: Annual Reviews 4139 El Camino Way, PO Box 10139, Palo Alto, CA 94303-0139, USA, 423–447.

[18] Christensen, O. B., and Christensen, J. H. (2004). Intensification of extreme European summer precipitation in a warmer climate. *Global and Planetary Change 44*, ISBN: 0921-8181 Publisher: Elsevier, 107–117.

[19] Classen, A. T., Sundqvist, M. K., Henning, J. A., Newman, G. S., Moore, J. A., Cregger, M. A., Moorhead, L. C., and Patterson, C. M. (2015). Direct and indirect effects of climate change on soil microbial and soil microbial-plant interactions: What lies ahead? *Ecosphere 6*, ISBN: 2150-8925 Publisher: Wiley Online Library, 1–21.

[20] Dieleman, W. I. J., Vicca, S., Dijkstra, F. A., Hagedorn, F., Hovenden, M. J., Larsen, K. S., Morgan, J. A., Volder, A., Beier, C., Dukes, J. S., King, J., Leuzinger, S., Linder, S., Luo, Y., Oren, R., De Angelis, P., Tingey, D., Hoosbeek, M. R., and Janssens, I. A. (2012). Simple additive effects are rare: a quantitative review of plant biomass and soil process responses to combined manipulations of CO2 and temperature. *Global Change Biology 18*, 2681–2693.

[21] Feofilova, E. P., Ivashechkin, A. A., Alekhin, A. I., and Sergeeva, Y. E. (2012). Fungal spores: Dormancy, germination, chemical composition, and role in biotechnology (review). *Applied Biochemistry and Microbiology 48*, 1–11.

[22] Friedlingstein, P. et al. (2023). Global Carbon Budget 2023. *Earth System Science Data 15*, Publisher: Copernicus GmbH, 5301–5369.

[23] Gorka, S., Darcy, S., Horak, J., Imai, B., Mohrlok, M., Salas, E., Richter, A., Schmidt, H., Wanek, W., Kaiser, C., and Canarini, A. (2023). Beyond PLFA: Concurrent extraction of neutral and glycolipid fatty acids provides new insights into soil microbial communities. *Soil Biology and Biochemistry 187*, 109205.

[24] Gulev, S. K., Thorne, P. W., Ahn, J., Dentener, F. J., Domingues, C. M., Gerland, S., Gong, D., Kaufman, D. S., Nnamchi, H. C., and Quaas, J. (2021). Changing state of the climate system. Publisher: Cambridge University Press.

[25] Hayden, H. L., Mele, P. M., Bougoure, D. S., Allan, C. Y., Norng, S., Piceno, Y. M., Brodie, E. L., DeSantis, T. Z., Andersen, G. L., and Williams, A. L. (2012). Changes in the microbial community structure of bacteria, archaea and fungi in response to elevated CO2 and warming in an A ustralian native grassland soil. *Environmental microbiology 14*, ISBN: 1462-2912 Publisher: Wiley Online Library, 3081–3096.

[26] He, Z., Xu, M., Deng, Y., Kang, S., Kellogg, L., Wu, L., Van Nostrand, J. D., Hobbie, S. E., Reich, P. B., and Zhou, J. (2010). Metagenomic analysis reveals a marked divergence in the structure of belowground microbial communities at elevated CO2. *Ecology Letters 13*, 564–575.

[27] Ingraham, N. L., and Criss, R. E. (1993). Effects of surface area and volume on the rate of isotopic exchange between water and water vapor. *Journal of Geophysical Research: Atmospheres 98*, ISBN: 0148-0227 Publisher: Wiley Online Library, 20547–20553.

[28] Jansson, J. K., and Hofmockel, K. S. (2020). Soil microbiomes and climate change. *Nature Reviews Microbiology 18*, Publisher: Nature Publishing Group, 35–46.

[29] Jennings, D. H. (1990). The ability of Basidiomycete mycelium to move nutrients through the soil ecosystem. ISBN: 1851663886.

[30] Joergensen, R. G., and Mueller, T. (1996). The fumigation-extraction method to estimate soil microbial biomass: calibration of the kEN value. *Soil biology and biochemistry 28*, ISBN: 0038-0717 Publisher: Elsevier, 33–37.

[31] Jones, S. E., and Lennon, J. T. (2010). Dormancy contributes to the maintenance of microbial diversity. *Proceedings of the National Academy of Sciences 107*, ISBN: 0027-8424 Publisher: National Acad Sciences, 5881–5886.

[32] Kaisermann, A., de Vries, F. T., Griffiths, R. I., and Bardgett, R. D. (2017). Legacy effects of drought on plant–soil feedbacks and plant–plant interactions. *New Phytologist 215*, 1413–1424.

[33] Kallenbach, C. M., Frey, S. D., and Grandy, A. S. (2016). Direct evidence for microbial-derived soil organic matter formation and its ecophysiological controls. *Nature communications 7*, ISBN: 2041-1723 Publisher: Nature Publishing Group UK London, 13630.

[34] Köchy, M., Hiederer, R., and Freibauer, A. (2015). Global distribution of soil organic carbon–Part 1: Masses and frequency distributions of SOC stocks for the tropics, permafrost regions, wetlands, and the world. *Soil 1*, ISBN: 2199-3971 Publisher: Copernicus GmbH, 351–365.

[35] Kourmentza, C., Plácido, J., Venetsaneas, N., Burniol-Figols, A., Varrone, C., Gavala, H. N., and Reis, M. A. (2017). Recent advances and challenges towards sustainable polyhydroxyalkanoate (PHA) production. *Bioengineering 4*, ISBN: 2306-5354 Publisher: MDPI, 55.

[36] Lê, S., Josse, J., and Husson, F. (2008). FactoMineR: an R package for multivariate analysis. *Journal of statistical software 25*, ISBN: 1548-7660, 1–18.

[37] Lehmann, J., and Kleber, M. (2015). The contentious nature of soil organic matter. *Nature 528*, ISBN: 0028-0836 Publisher: Nature Publishing Group UK London, 60–68.

[38] Liang, C., Schimel, J. P., and Jastrow, J. D. (2017). The importance of anabolism in microbial control over soil carbon storage. *Nature microbiology 2*, ISBN: 2058-5276 Publisher: Nature Publishing Group, 1–6.

[39] Manzoni, S., Ding, Y., Warren, C., Banfield, C. C., Dippold, M. A., and Mason-Jones, K. (2021). Intracellular storage reduces stoichiometric imbalances in soil microbial biomass–A theoretical exploration. *Frontiers in*

Ecology and Evolution 9, ISBN: 2296-701X Publisher: Frontiers Media SA, 714134.

[40] Manzoni, S., Taylor, P., Richter, A., Porporato, A., and Ågren, G. I. (2012). Environmental and stoichiometric controls on microbial carbon-use efficiency in soils. *New Phytologist 196*, ISBN: 0028-646X Publisher: Wiley Online Library, 79–91.

[41] Mason-Jones, K., Breidenbach, A., Dyckmans, J., Banfield, C. C., and Dippold, M. A. (2023). Intracellular carbon storage by microorganisms is an overlooked pathway of biomass growth. *Nature Communications 14*, ISBN: 2041-1723 Publisher: Nature Publishing Group UK London, 2240.

[42] Mason-Jones, K., Robinson, S. L., Veen, G. F., Manzoni, S., and van der Putten, W. H. (2022). Microbial storage and its implications for soil ecology. *The ISME Journal 16*, ISBN: 1751-7362 Publisher: Oxford University Press, 617–629.

[43] Masson-Delmotte, V. P., Zhai, P., Pirani, S. L., Connors, C., Péan, S., Berger, N., Caud, Y., Chen, L., Goldfarb, M. I., and Scheel Monteiro, P. M. (2021). Ipcc, 2021: Summary for policymakers. in: Climate change 2021: The physical science basis. contribution of working group i to the sixth assessment report of the intergovernmental panel on climate change. Publisher: Cambridge University Press, Cambridge, United Kingdom and New York, NY, USA.

[44] McDonald, M. D., Owusu-Ansah, C., Ellenbogen, J. B., Malone, Z. D., Ricketts, M. P., Frolking, S. E., Ernakovich, J. G., Ibba, M., Bagby, S. C., and Weissman, J. L. (2024). What is microbial dormancy? *Trends in Microbiology 32*, Publisher: Elsevier, 142–150.

[45] Metze, D., Schnecker, J., de Carlan, C. L. N., Bhattarai, B., Verbruggen, E., Ostonen, I., Janssens, I. A., Sigurdsson, B. D., Hausmann, B., and Kaiser, C. (2024). Soil warming increases the number of growing bacterial taxa but

not their growth rates. *Science Advances 10*, ISBN: 2375-2548 Publisher: American Association for the Advancement of Science, eadk6295.

[46] Moanis, R., Geeraert, H., Van den Brande, N., Hennecke, U., and Peeters, E. (2024). Paracoccus kondratievae produces poly (3-hydroxybutyrate) under elevated temperature conditions. *Environmental Microbiology Reports 16*, ISBN: 1758-2229 Publisher: Wiley Online Library, e13260.

[47] Mooshammer, M., Wanek, W., Hämmerle, I., Fuchslueger, L., Hofhansl, F., Knoltsch, A., Schnecker, J., Takriti, M., Watzka, M., and Wild, B. (2014). Adjustment of microbial nitrogen use efficiency to carbon: nitrogen imbalances regulates soil nitrogen cycling. *Nature communications 5*, ISBN: 2041-1723 Publisher: Nature Publishing Group UK London, 3694.

[48] Moyano, F. E., Manzoni, S., and Chenu, C. (2013). Responses of soil heterotrophic respiration to moisture availability: An exploration of processes and models. *Soil Biology and Biochemistry 59*, ISBN: 0038-0717 Publisher: Elsevier, 72–85.

[49] Murphy, D. J. (2012). The dynamic roles of intracellular lipid droplets: from archaea to mammals. *Protoplasma 249*, Springer, 541–585.

[50] Naylor, D., DeGraaf, S., Purdom, E., and Coleman-Derr, D. (2017). Drought and host selection influence bacterial community dynamics in the grass root microbiome. *The ISME Journal 11*, 2691–2704.

[51] Naylor, D., Sadler, N., Bhattacharjee, A., Graham, E. B., Anderton, C. R., McClure, R., Lipton, M., Hofmockel, K. S., and Jansson, J. K. (2020). Soil microbiomes under climate change and implications for carbon cycling. *Annual Review of Environment and Resources 45*, ISBN: 1543-5938 Publisher: Annual Reviews, 29–59.

[52] Oksanen, J., Blanchet, F. G., Kindt, R., Legendre, P., Minchin, P., O'Hara, R., Simpson, G., Solymos, P., Stevens, M., and Wagner, H. vegan Community Ecology Package. Vienna, Austria, 2012.

[53] Olsson, P. A., and Johansen, A. (2000). Lipid and fatty acid composition of hyphae and spores of arbuscular mycorrhizal fungi at different growth stages. *Mycological Research 104*, 429–434.

[54] Olsson, P. A., and Lekberg, Y. (2022). A critical review of the use of lipid signature molecules for the quantification of arbuscular mycorrhiza fungi. *Soil Biology and Biochemistry 166*, 108574.

[55] Oren, A. (1999). Bioenergetic aspects of halophilism. *Microbiology and molecular biology reviews 63*, ISBN: 1098-5557 Publisher: Am Soc Microbiol, 334–348.

[56] Pinheiro, J., and Bates, D. nlme Linear and Nonlinear Mixed Effects Models, 2023.

[57] Poblete-Castro, I., Escapa, I. F., Jäger, C., Puchalka, J., Chi Lam, C. M., Schomburg, D., Prieto, M. A., and Martins dos Santos, V. A. (2012). The metabolic response of P. putida KT2442 producing high levels of polyhydroxyalkanoate under single-and multiple-nutrient-limited growth: Highlights from a multi-level omics approach. *Microbial cell factories 11*, Publisher: Springer, 1–21.

[58] Raumberg-Gumpenstein Klimafolgenforschung an der HBLFA Raumberg-Gumpenstein ClimGrass, https://raumberg-gumpenstein.at [25.08.2024].

[59] Ren, C., Chen, J., Lu, X., Doughty, R., Zhao, F., Zhong, Z., Han, X., Yang, G., Feng, Y., and Ren, G. (2018). Responses of soil total microbial biomass and community compositions to rainfall reductions. *Soil Biology and Biochemistry 116*, 4–10.

[60] Rillig, M. C., Ryo, M., Lehmann, A., Aguilar-Trigueros, C. A., Buchert, S., Wulf, A., Iwasaki, A., Roy, J., and Yang, G. (2019). The role of multiple global change factors in driving soil functions and microbial biodiversity. *Science 366*, ISBN: 0036-8075 Publisher: American Association for the Advancement of Science, 886–890.

[61] Ruiz, J. A., López, N. I., Fernández, R. O., and Méndez, B. S. (2001). Polyhydroxyalkanoate degradation is associated with nucleotide accumulation and enhances stress resistance and survival of Pseudomonas oleovorans in natural water microcosms. *Applied and Environmental Microbiology 67*, ISBN: 1098-5336 Publisher: Am Soc Microbiol, 225–230.

[62] Schimel, J., Balser, T. C., and Wallenstein, M. (2007). Microbial stress-response physiology and its implications for ecosystem function. *Ecology 88*, ISBN: 1939-9170 Publisher: Wiley Online Library, 1386–1394.

[63] Schimel, J. P. (2018). Life in dry soils: effects of drought on soil microbial communities and processes. *Annual review of ecology, evolution, and systematics 49*, ISBN: 1543-592X Publisher: Annual Reviews, 409–432.

[64] Schimel, J. P., and Schaeffer, S. M. (2012). Microbial control over carbon cycling in soil. *Frontiers in microbiology 3*, ISBN: 1664-302X Publisher: Frontiers Research Foundation, 348.

[65] Schmidt, M. W., Torn, M. S., Abiven, S., Dittmar, T., Guggenberger, G., Janssens, I. A., Kleber, M., Kögel-Knabner, I., Lehmann, J., and Manning, D. A. (2011). Persistence of soil organic matter as an ecosystem property. *Nature 478*, ISBN: 0028-0836 Publisher: Nature Publishing Group UK London, 49–56.

[66] Sherwood, S., and Fu, Q. (2014). A Drier Future? *343*, 737–739.

[67] Shukla, P. R., Skeg, J., Buendia, E. C., Masson-Delmotte, V., Pörtner, H.-O., Roberts, D. C., Zhai, P., Slade, R., Connors, S., and Van Diemen, S. (2019). Climate Change and Land: an IPCC special report on climate change, desertification, land degradation, sustainable land management, food security, and greenhouse gas fluxes in terrestrial ecosystems.

[68] Six, J., Frey, S. D., Thiet, R. K., and Batten, K. M. (2006). Bacterial and fungal contributions to carbon sequestration in agroecosystems. *Soil Science*

Society of America Journal 70, ISBN: 0361-5995 Publisher: Wiley Online Library, 555–569.

[69] Smith, S. E., and Read, D. J., *Mycorrhizal symbiosis*; Academic press: 2010.

[70] Song, J. et al. (2019). A meta-analysis of 1,119 manipulative experiments on terrestrial carbon-cycling responses to global change. *Nature Ecology & Evolution 3*, Publisher: Nature Publishing Group, 1309–1320.

[71] Soong, J. L., Fuchslueger, L., Marañon-Jimenez, S., Torn, M. S., Janssens, I. A., Penuelas, J., and Richter, A. (2020). Microbial carbon limitation: The need for integrating microorganisms into our understanding of ecosystem carbon cycling. *Global change biology 26*, ISBN: 1354-1013 Publisher: Wiley Online Library, 1953–1961.

[72] Steinbüchel, A. (2001). Perspectives for biotechnological production and utilization of biopolymers: metabolic engineering of polyhydroxyalkanoate biosynthesis pathways as a successful example. *Macromolecular Bioscience 1*, ISBN: 1616-5187 Publisher: Wiley Online Library, 1–24.

[73] Stevenson, A., and Hallsworth, J. E. (2014). Water and temperature relations of soil A ctinobacteria. *Environmental microbiology reports 6*, ISBN: 1758-2229 Publisher: Wiley Online Library, 744–755.

[74] Tao, F., Huang, Y., Hungate, B. A., Manzoni, S., Frey, S. D., Schmidt, M. W., Reichstein, M., Carvalhais, N., Ciais, P., and Jiang, L. (2023). Microbial carbon use efficiency promotes global soil carbon storage. *Nature*, ISBN: 0028-0836 Publisher: Nature Publishing Group UK London, 1–5.

[75] Team, R. C. R A Language and Environment for Statistical Computing, Vienna, Austria, 2023.

[76] US Department of Commerce, N. Global Monitoring Laboratory - Carbon Cycle Greenhouse Gases, EN-US, 2024.

[77] Vance, E. D., Brookes, P. C., and Jenkinson, D. S. (1987). An extraction method for measuring soil microbial biomass C. *Soil biology and Biochemistry 19*, ISBN: 0038-0717 Publisher: Elsevier, 703–707.

[78] Varpe, Ø., and Ejsmond, M. J. (2018). Trade-offs between storage and survival affect diapause timing in capital breeders. *Evolutionary ecology 32*, ISBN: 0269-7653 Publisher: Springer, 623–641.

[79] Walker, T. W., Kaiser, C., Strasser, F., Herbold, C. W., Leblans, N. I., Woebken, D., Janssens, I. A., Sigurdsson, B. D., and Richter, A. (2018). Microbial temperature sensitivity and biomass change explain soil carbon loss with warming. *Nature climate change 8*, ISBN: 1758-6798 Publisher: Nature Publishing Group, 885–889.

[80] Wang, C., Qu, L., Yang, L., Liu, D., Morrissey, E., Miao, R., Liu, Z., Wang, Q., Fang, Y., and Bai, E. (2021). Large-scale importance of microbial carbon use efficiency and necromass to soil organic carbon. *Global Change Biology 27*, ISBN: 1354-1013 Publisher: Wiley Online Library, 2039–2048.

[81] Watzer, B., and Forchhammer, K., *Cyanophycin: a nitrogen-rich reserve polymer*; UK: IntechOpen: 2018.

[82] Werker, A., Lind, P., Bengtsson, S., and Nordström, F. (2008). Chlorinated-solvent-free gas chromatographic analysis of biomass containing polyhydroxyalkanoates. *Water Research 42*, 2517–2526.

[83] White, R. P., Murray, S., Rohweder, M., Prince, S. D., and Thompson, K. M. (2000). Grassland ecosystems. *World Resources Institute: Washington, DC, USA 81*.

[84] Wickham, H., *ggplot2: Elegant Graphics for Data Analysis*; Springer-Verlag New York: 2016.

[85] Wood, J. M. (2015). Perspectives on: the response to osmotic challenges: bacterial responses to osmotic challenges. *The Journal of general physiology 145*, Publisher: The Rockefeller University Press, 381.

[86] Xu, Z., Jiang, Y., Jia, B., and Zhou, G. (2016). Elevated-CO2 response of stomata and its dependence on environmental factors. *Frontiers in plant science 7*, ISBN: 1664-462X Publisher: Frontiers, 169580.